RrLHY regulates arginine biosynthesis by activating *RrNAGS1* in *Rosa roxburghii* fruit

Xufeng Yang[a, b], Nanyu Li[a], Richard Ludlow[c], Qianmin Hua[a], Zhaoxin Wu[a], Qinqian[a] Yuan, Zhifa Li[a], Min Lu[a, *], Huaming An[b, *]

[a] *Agricultural College, Guizhou University, Guiyang, 550025, People's Republic of China*

[b] *Engineering Research Center of National Forestry and Grassland Administration for Rosa roxburghii*

[c] *School of Biosciences, Cardiff University, Sir Martin Evans Building, Museum Avenue, Cardiff, UK*

[*]Author for correspondence: mlv@gzu.edu.cn; hman@gzu.edu.cn

Abstract

As a semi-essential amino acid, arginine is crucial for human health and a key determinant of the nutritional quality of *Rosa roxburghii* fruits. We explore the regulatory dynamics of arginine metabolism in *R. roxburghii* fruits, with a focus on the key genes and transcription factors involved in this process. The content of arginine exhibits significant fluctuations during fruit maturation, peaking at 60 days after anthesis (DAA) before declining. Genome-wide and transcriptomic analyses of *R. roxburghii* have identified 21 genes involved in arginine synthesis and four genes related to arginine catabolism. Notably, N-acetylglutamate synthetase (*RrNAGS1)* and arginine decarboxylase *(RrADC1*) show a strong correlation with arginine content. Overexpression studies of *RrNAGS1* and *RrADC1* have confirmed their roles in regulating arginine levels, with *RrNAGS1* promoting and *RrADC1* inhibiting arginine accumulation. Additionally, Late Elongated Hypocotyl (RrLHY), a nucleus-localized MYB transcription factor, directly binds to and activates the *RrNAGS1* promoter, thereby significantly influencing arginine biosynthesis in *R. roxburghii* fruits, as demonstrated by both overexpression and gene silencing studies. These findings provide valuable insights into the molecular mechanisms governing arginine accumulation in fruit and offer potential strategies for the targeted manipulation of arginine levels in crop species.

Key words: Arginine; *Rosa roxburghii* Tratt; *RrNAGS1*; *RrADC1*; RrLHY

1. Introduction

Rosa roxburghii Tratt, a member of the *Rosaceae* family, is a plant of considerable value for both medicinal and applications (Shen et al., 2023). In China, particularly in the southwestern and south-central regions, this species has been extensively cultivated, with Guizhou Province recognized as its primary cultivation area (Yu et al., 2021). Data from 2022 indicates that over 80 counties and cities in

Guizhou Province are involved in the cultivation of *R. roxburghii*. This cultivation spans an area of 140,000 hectares and yields an annual production of 300,000 tons, contributing an industry value exceeding 15 billion yuan to the local economy (Liu, 2022). The fruit of *R. roxburghii* is highly nutritious, containing substantial amounts of vitamin C, antioxidants, polysaccharides, dietary fiber, and amino acids, among other components. These nutrients provide significant health benefits, including hypoglycemic, hypolipidemic, radioprotective, antitoxic, and anticancer properties (Jain et al., 2024; Yin et al., 2024). Additionally, the roots and leaves of *R. roxburghii* are employed in traditional medicine for the treatment of diarrhea and indigestion, respectively (Wu et al., 2021). The unique health benefits of *R. roxburghii* have made it sought after in the market for functional foods and health supplements, demonstrating promising prospects for clinical applications (Wang et al., 2021).

Arginine is an important multifunctional semi-essential amino acid found in the fruit of *R. roxburghii*, which promotes urea synthesis, reduces cardiovascular mortality, supports the immune system, reduces male infertility, supports visual function, promotes cell proliferation, and accelerates wound healing processes (Zhang et al., 2018; Hiratsu et al., 2022; Dai et al., 2021; Wu et al., 2021; McKay et al., 2021; Reis et al., 2018). Additionally, arginine possesses anti-fatigue, anti-inflammatory, and anti-aging effects (Wang et al., 2015; Tran et al., 2020; He et al., 2024). As public awareness of health continues to rise, arginine has emerged as a significant nutritional supplement, and continues to see growing demand in the dietary supplement, health care product, and sports nutrition sectors. Notably, the utilization of arginine by athletes and fitness enthusiasts has further driven market demand (Gambardella et al., 2021). Among fruits, most contain arginine at levels ranging from 20 to 35 mg / 100 g. However, the arginine content in the fruit of *R. roxburghii* is significantly higher than that found in common fruits, reaching 66 mg / 100 g (Lu et al., 2017; Lv et al., 2023).

The accumulation of arginine in plants is regulated by anabolism and catabolism. In the anabolic pathway, glutamate is converted into arginine through a series of enzyme-catalyzed reactions. This process involves several key enzymes, including N-acetylglutamate synthase (NAGS), N-acetylglutamate kinase (NAGK), ornithine transcarbamylase (OTC), argininosuccinate synthetase (ASS), and argininosuccinate lyase (ASL) (Slocum, 2005; Winter et al., 2015). Conversely, arginine is catabolized through three primary metabolic pathways, resulting in the production of polyamines (PAs) or nitric oxide (NO). This catabolic process is regulated by three key enzymes: arginase, nitric oxide synthase (NOS), and arginine decarboxylase (ADC) (Satriano et al., 2004). Numerous plants have been

identified as possessing genes that encode enzymes involved in arginine metabolic enzymes, however, it is noteworthy that the genes for key enzymes in arginine metabolism differ between plant species. In peanuts (*Arachis hypogaea* L.), the key gene responsible for arginine biosynthesis encodes *ASS* (Li et al., 2022). Meanwhile, in the development of watermelon (*Citrullus lanatus*) fruit peel, *OTC* plays a crucial role (Joshi et al., 2019). In rice (*Oryza sativa*), mutations in the *ASL* gene significantly affect both arginine content and root growth (Xia et al., 2014a).

Additionally, arginine metabolism is regulated by numerous transcription factors. For instance, SlMYC2 mediates the effect of MeJA on arginine metabolism (Min, 2019), and ATF-4 activates the *ASS* gene to regulate arginine content in peanuts (Li et al., 2022). Similarly, CsCBF1 controls *CsADC* expression and Put synthesis, enhancing cold resistance in plants (Song et al., 2022). Moreover, AbbHLH1 regulates arginine metabolism genes in the cultivated mushroom (*Agaricus bisporus*), controlling postharvest development (Wang et al., 2023). Currently, no genes related to arginine metabolic enzymes have been identified in *R. roxburghii*. The exploration of key regulatory genes for arginine in the fruit of *R. roxburghii* is of great significance for improving the fruit quality and optimizing amino acid composition.

This study assessed the variations in arginine content across eight critical developmental stages, from post-anthesis to maturation, in *R. roxburghii* fruit, utilizing an amino acid analyzer. Additionally, by integrating transcriptomic and genomic data from *R. Roxburghii*, we elucidate the key genes that influence arginine content in the fruit, along with their regulatory mechanisms. In summary, this study examined the accumulation patterns, biosynthetic and catabolic pathways, and the transcriptional regulatory network of arginine in the fruit of *R. roxburghii*. These results provide new insights into the potential applications of *R. roxburghii* fruit in the food industry and pharmaceutical sector.

2. Materials and Methods

2.1 Plant materials and growth conditions

The plant materials used in this study included *R. roxburghii* ‘Guinong 5’, tobacco (*Nicotiana tabacum*), and strawberry (*Fragaria* × *ananassa*). The *R. roxburghii* plants used in this study were six-year-old agamic trees of ‘Guinong 5’ and were grown at the Department of Horticulture, Guizhou University (26°42.408’N, 106°67.353’E). Fruits were collected every 15 days from May 15th (15 days after anthesis, 15 DAA) until maturity (120 DAA). During the collection process, we also measured the single fruit weight of each sample. A portion of the fruits were frozen immediately in liquid nitrogen and

stored at -80 °C to study the expression of arginine-related genes, and the other portion was washed with deionized water and then dried at 55 °C until a constant weight was obtained. The dried samples were ground in a pestle and mortar, then passed through a 65-mesh screen for amino acid analysis. Tobacco plants were cultivated under the following conditions: a light/dark cycle of 16/8 hours, day/night temperatures of 25/20 ℃, humidity of 70 %, and a light intensity of 200 PPFD. Strawberries were cultivated in greenhouses under ambient conditions.

2.2 Measurement of amino acids content in plants

The determination of hydrolyzed and free amino acids in *R. roxburghii* fruit was carried out following the methods outlined by Gehrke et al. (1985) and Lu et al. (2020), with minor modifications. To measure hydrolyzed amino acids, 1 g of dried *R. roxburghii* fruit sample, which had been sieved through a 60-mesh screen, was extracted using 50 mL of 0.01 mol/L hydrochloric acid for a duration of 30 minutes, followed by filtration. Subsequently, 2 ml of the filtrate was combined with 2 ml of 8% sulfosalicylic acid and allowed to stand for 15 min. The mixture was then centrifuged at 10,000 rpm for 10 min. The supernatant was filtered through a 0.45 μm or 0.22 μm filter membrane and transferred into a 1.5 mL sample vial. The measurement of free amino acids involves weighing 150 mg of dried *R. roxburghii* fruit powder that has been sieved through a 60-mesh screen. Subsequently, 5 mL of 6 mol/L hydrochloric acid and 1-2 drops of phenol are added to the powder. The resulting mixture is then hydrolyzed at 110 °C for 24 hours. After hydrolysis is complete, the solution is allowed to cool, and its volume is adjusted to 100 mL with distilled water, while the pH is concurrently adjusted to 2. Following this, the mixture is filtered, and the filtrate is collected in a 1.5 mL sample vial. Both procedures employ the S-433D Automatic Amino Acid Analyzer for quantification.

2.3 Determination of NAGS enzyme activity and ADC enzyme activity

Based on the principle of enzyme-linked immunosorbent assay (ELISA), the N-acetylglutamate synthase (NAGS) ELISA kit (ML-E-23951) and Arginine decarboxylase (ADC) ELISA kit (ML-E-23828-1) from Shanghai ML Biotech Co., Ltd. were used for determination.

2.4 DNA, RNA extraction and Quantitative reverse transcription PCR (qRT-PCR) analysis

Plant DNA was extracted from leaves using a novel rapid plant genome DNA extraction kit (Bio Teke Corporation), in accordance with the manufacturer's instructions. Total RNA from *R. roxburghii* samples was extracted following the guidelines provided by the MiniBEST Plant RNA Extraction Kit (Takara, Japan). Subsequently, 1 μg of the total RNA was utilized for cDNA synthesis, using the

PrimeScript RT reagent kit along with the gDNA Eraser Kit (Perfect Real Time, Takara). Primer design and synthesis were completed by Sangon Biotech Co., Ltd. (Shanghai, China), while specific primers for the housekeeping genes ubiquitin (*RrUBQ*) and glyceraldehyde-3-phosphate dehydrogenase (*RrGAPDH*) as internal controls were those reported by Lu et al. (2020). qRT-PCR was conducted following the TB Green Premix EX TaqII (Tli RNaseH Plus) kit instructions. The reaction program was as follows: (1) 95 °C for 30 s; (2) 40 cycles of 95 °C for 5 s, 55 °C-60 °C for 20 s, and 72 °C for 20 s; (3) a melt curve program of 95 °C for 15 s, a temperature increase from 55 °C to 95 °C in increments of 0.3 °C/min, and 95 °C for 15 s. Finally, the relative expression was calculated by the $2^{-\Delta\Delta CT}$ method. qRT-PCR reactions for at least three biological replicates, each consisting of three technical replicates, utilizing a real-time PCR detection system. The primers used are listed in Supplemental Table S1.

2.5 Construction of vectors and transformation of *R. roxburghii* and Strawberry

To construct overexpressing vectors for *RrNAGS1*, *RrADCl*, and *RrLHY*, the coding sequences of these genes were amplified by PCR using gene-specific primers (Table S1). These sequences were then inserted into the polylinker sites of the pCAMBIA 1301 vector, which is regulated by the CaMV 35S promoter (Fig. S1). The empty pCAMBIA 1301 vector served as a control. The recombinant vectors were introduced into *Agrobacterium tumefaciens* strain GV3101 by heat shock after verification by sequencing. In the transient transformation experiment, we injected an Agrobacterium suspension (OD600 0.8-1.0) containing 10 mM MES, 10 mM $MgCl_2$, and 200 μM AS into *R. roxburghii* fruits at 60 DAA and into strawberries at the white-ripe stage. The experiment included four groups, each containing a minimum of 30 *R. roxburghii* and strawberry fruits. Each fruit underwent three injections, spaced four days apart. After a period of 20 days, samples were collected for gene expression analysis and to assess arginine content. For the transformation of *R. roxburghii* callus, the callus was incubated in a suspension of transformed *Agrobacterium tumefaciens* (OD600 = 0.6) containing 200 μM AS, and shaken for 20 min at 200 rpm and 28 °C. Subsequently, the callus was washed with 300 mg/mL cephalosporin and then with sterilized water, followed by a 2-day co-incubation period in the dark. Finally, the callus was inoculated onto a culture medium containing 5 mg/L hygromycin for positive callus screening. The callus was cultivated in an incubator under 230 PPFD light intensity, and the callus was collected at 6 pm after 40 days for gene expression analysis and arginine determination.

To achieve the silencing of the *RrNAGS1*, *RrADCl*, and *RrLHY* genes in *R. roxburghii* fruits, the coding sequences of *RrNAGS1*, *RrADCl*, and *RrLHY* were amplified using gene-specific primers via

PCR (Table S1). This amplified fragment was subsequently inserted into the polylinker sites (EcoR I/BamH I) of the pTRV2 vector, which is regulated by the CaMV 35S promoter (Fig. S1). The unaltered pTRV2 vector served as a control. Following verification by sequencing, the recombinant vectors were introduced into the *Agrobacterium tumefaciens* strain GV3101 using a heat shock method. The suspension of transformed *Agrobacterium tumefaciens*, containing both pTRV1 and the target gene pTRV2, was combined in a 1:1 ratio prior to injection. *R. roxburghii* fruits, at 60 (DAA), were injected with the transformed *Agrobacterium tumefaciens* suspension (OD600 = 1.6-2.0), which included 10 mM MES, 10 mM MgCl2, and 200 μM AS. Four groups were injected, with each group comprising no fewer than 30 *R. roxburghii* fruits. Samples were collected 20 days post-injection for gene expression analysis and arginine determination.

2.6 Subcellular localization analysis

The full-length *RrLHY* coding sequences without stop codons were ligated into the pCAMBIA35S-EGFP vector. A list of the primers utilized for vector construction can be found in Supplemental Table S1. After electroporation into *Agrobacterium tumefaciens* GV3101, the recombinant vectors were transiently expressed in tobacco leaves. The *A. tumefaciens* culture was adjusted to an OD600 of 0.5 with the infiltration buffer, which contained 10 mM MES, 10 mM $MgCl_2$, and 150 mM acetosyringone at a pH of 5.6. Using a confocal laser scanning microscope (LSM510, Carl Zeiss, Germany), GFP fluorescence was measured and observed 2 days after infiltration. The excitation wavelength for GFP fluorescence was 488 nm, and fluorescence was detected between 490 and 520 nm. The excitation wavelength for NLS fluorescence was 594 nm, and fluorescence was detected between 612 and 635 nm.

2.7 Dual-luciferase assay

The dual-luciferase assay was performed as per Fan et al. (2024), albeit with some minor adjustments to cater to our specific experimental needs. The full-length cDNA of *RrLHY* was cloned into the pCAMBIA 1301 vector. This was accomplished using the restriction enzyme sites *Kpn*I (GGTACC) and *MIuI*, resulting in the creation of an effector construct, as illustrated in Supplemental Figure S1. For the preparation of a reporter construct, various fragments of the *RrNAGS1* promoter were inserted upstream of the LUC reporter gene within the pGreenII 0800-LUC vector using *Kpn*I and *Eco*RV restriction enzyme sites (Fig. S1). GV3101 of *A. tumefaciens* was electroporated with each of the reporter and effector constructs and subsequently suspended in the same infiltration buffer used in the subcellular localization analysis, with an OD600 of 0.5. tobacco leaves were infiltrated with *A. tumefaciens*

combinations of promoters and transcription factors (TFs) at a ratio of 1:9 using needleless syringes. The LUC/REN fluorescence was evaluated using the Dual Luciferase Reporter Assay System (Promega, Madison, USA) three days post-infiltration. Each TF-promoter interaction experiment included three biological replicates.

2.8 Yeast 1-hybrid assay

The Y1H assay method was conducted as described by Gao et al. (2021), with minor modifications. The interaction of *RrLHY* with the promoters of *RrNAGS1* and *RrADC1* was assessed using the Matchmaker Gold Yeast One-Hybrid Library Screening System (Clontech, Mountain View, California). The 2-kb promoter sequence of *RrNAGS1* and *RrADC1* were cloned into the *EcoR*I and *BamH*I restriction sites of the pAbAi vector, which functioned as the bait for screening the library. cDNA of *RrLHY* was obtained through PCR amplification from *R. roxburghii* and subsequently cloned into a pGADT7 vector using the *EcoR*I and *BamH*I restriction sites. The transformed pHIS2 bait vector and pGADT7 prey vector were introduced into Y187 yeast cells, which were subsequently cultured on SD/-Trp/-Leu/-His medium. After 3 days, positive yeast colonies were selected and diluted in sterile distilled water to achieve an optical density at 600 nm (OD600) of 0.15-0.3. A volume of 2.5 μl from this suspension was then spotted onto SD/-Trp/-Leu/-His plates, with or without the addition of 3-AT. The plates were incubated at 30 ℃ for 5-7 days. All primers utilized in this study are listed in Supplemental Table S1.

2.9 Electrophoretic mobility shift assay

The full-length *RrLHY* gene was inserted into the pMAL vector to produce MBP-tagged fusion proteins. The resulting recombinant construct was then transformed into *Escherichia coli* BL21 (DE3) and purified. The expression and purification of the recombinant *RrLHY*-His protein was performed using the methodology described by Kyung et al. (2022). The LightShift Chemiluminescent EMSA Kit (ThermoFisher Scientific, Waltham, MA, USA) was used following the manufacturer's instructions. Twenty-base-pair sequences containing the AAATAT motif, derived from the *RrNAGS1* promoter, were labeled with 5′ biotin by HuaGene. Unlabeled DNA fragments identical to the probes were used as competitors (cold probes). In the mutant probes, the AAATAT motif in the DNA fragments was replaced with a polyC sequence. The detailed primer sequences are provided in Table S1.

2.10 Bioinformatic analysis

The MEGA 7.0 program (Kumar et al., 2016) was utilized to align the full-length amino acid

sequences of NAGS and ADC, as well as to construct a neighbor-joining phylogenetic tree. Furthermore, The cis-acting elements within the promoters of *RrNAGS1*, *RrADC1*, and *RrLHY* were predicted using the Plant CARE tool (available at https://bioinformatics.psb.ugent.be/webtools/plantcare/html/).

2.11 Statistical analysis

All experiments were conducted in triplicate, and the data are presented as means ± standard deviations. Statistical analyses were performed using SPSS 26.0 software (IBM, Armonk, NY, USA). Differences among mean values were assessed using one-way ANOVA, with a significance level set at $p < 0.05$, followed by Duncan's multiple range test. Graphs were generated using GraphPad Prism version 8.0, while TBtools software was employed for visualizing gene expression heat maps.

3. Results

3.1 Arginine accumulation in *R. roxburghii* fruit during development

From 15 days after anthesis (DAA), we collected fruits at eight developmental stages and measured their single-fruit weight (Fig. 1A). During the fruit development process, the single-fruit weight continued to increase (Fig. 1B). Total arginine consists of hydrolyzed arginine and free arginine. The trends of hydrolyzed arginine and free arginine in *R. roxburghii* fruit during development were similar, with the period from 45 to 60 days after flowering showing significant increase, and the 60 to 75 days period showing significant decrease. The content of free arginine and hydrolyzed arginine were highest at 60 DAA, reaching 414.70 mg/100g and 25.70 mg/100g, respectively. They were lowest at 75 DAA, at 4 mg/100g and 137.7 mg/100g, respectively (Fig. 1C). Furthermore, the study indicated that hydrolyzed glutamate and total hydrolyzed amino acids mirrored the trends of hydrolyzed arginine, underscoring the significant role of glutamate in arginine synthesis (Fig. 1D).

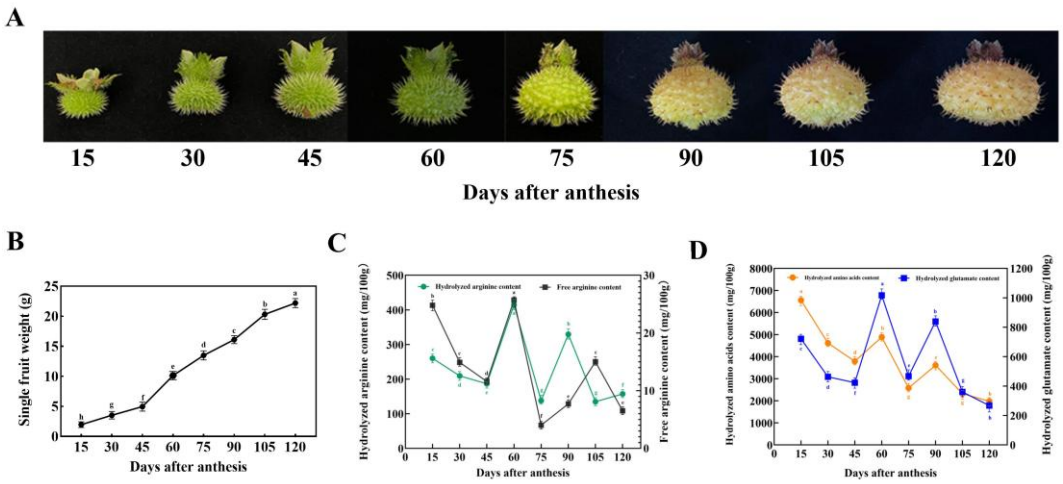

Fig.1. Changes of *R. roxburghii* fruits during the development.

(A) Photos of *R. roxburghii* fruits at different stages. (B) Dynamic changes in single fruit weight. (C) Arginine content in fruits at different development stages. (D) Total and hydrolyzed glutamate content in fruits at different development stages. Values are a mean of 3 replicates ± SD. Different lowercase letters indicate significant differences within each respective variable across DAA ($P<0.05$).

3.2 The expression of *RrNAGS1* and *RrADC1* correlates with the arginine content in fruit of *R. roxburghii*.

Based on the genome, there are a total of 34 structural genes involved in arginine synthesis and 8 major structural genes involved in degradation metabolism. By integrating transcriptomic data and excluding genes with no expression or expression levels below 1 at 30 DAA, 60 DAA, and 90 DAA, we identified that there are 21 genes involved in the arginine synthesis pathway, among which 2 genes as NAGS, 2 genes annotated to NAGK, 2 genes annotated to the ArgC, 3 genes annotated to ArgD, 3 genes annotated to ACY1, 3 genes annotated to ArgE, 4 genes annotated to ArgF, 3 genes annotated to ArgG and 1 gene annotated as ArgH. Additionally, there were 4 genes with expression involved in Arginine catabolism, including 1 annotated as NOS, 2 as ADC, and 1 as ARG (Table S2). Using qRT-PCR, we quantified the relative expression levels of these 21 synthetic metabolic genes (Fig.2A) and 4 degradation metabolic genes (Fig.2B) across 8 different developmental stages of 'Guinong 5' fruit and conducted correlation analysis with the contents of free arginine, hydrolyzed arginine, and total arginine (Table S2). The results indicate that the N-acetylglutamate synthetase (*RrNAGS1, evm.model.Contig273.43*) unigene is significantly positively correlated with the total arginine content ($R=0.834$, $P<0.01$; Fig. 2B), while the arginine decarboxylase (*RrADC1, evm.model.Contig284.256*) unigene is significantly negatively correlated with the total arginine content ($R = -0.646$, $P < 0.05$; Fig. 2D). This suggests that *RrNAGS1* and *RrADC1* play key roles in arginine synthesis and decomposition, respectively.

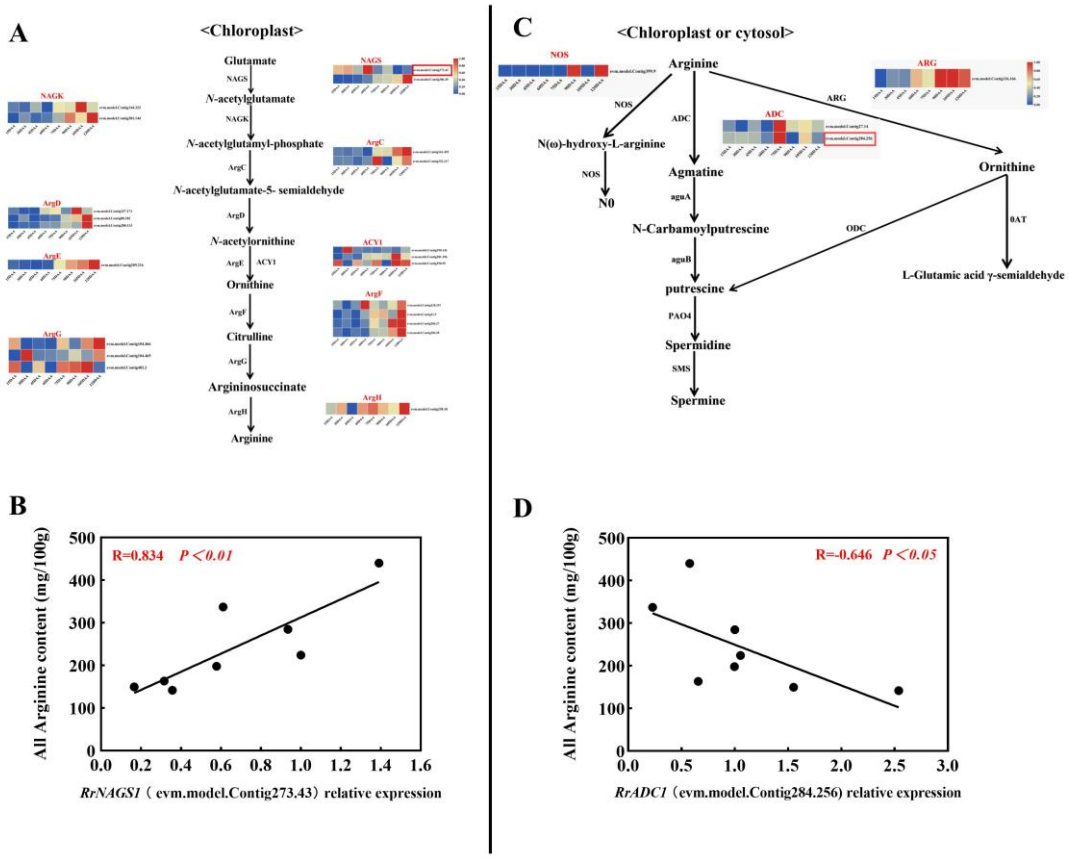

Fig.2. Gene expression of arginine metabolic pathways during eight developmental periods.

(A) Gene expression of the arginine synthesis pathway. (B) Correlation analysis between total arginine content and *RrNAGS1* expression. (C) Gene expression of the arginine decomposing pathway, (D) Correlation analysis between total arginine content and *RrADC1* expression. NAGS, N-acetylglutamate synthase; NAGK, N-acetylglutamate kinase; ArgC, N-acetylglutamatyl-5-P reductase; ArgD, N-acetylornithine aminotransferase; ACY1, N-acetylornithine-glutamate acetyltransferase; ArgE, N-acetylornithine deacetylase; ArgF, Ornithine transcarbamylase; ArgG, Argininosuccinate synthase; ArgH, Argininosuccinate lyase; NOS, Nitric oxide synthase; ADC, Arginine decarboxylase; aguA, Agmatinase; aguB, N-Carbamoylputrescine amidase; PAO4, Polyamine oxidase; SMS, Spermidine synthase; ODC, Ornithine decarboxylase; OTC, Ornithine transcarbamylase.

3.3 The overexpression and silencing effects of *RrNAGS1* and *RrADC1* in *R. roxburghii* fruit

To investigate the biological functions of *RrNAGS1* and *RrADC1* in fruit, we conducted transient overexpression experiments in *R. roxburghii* fruit. The findings indicate that, compared to the empty vector control, the expression level of *RrNAGS1* in OE-*RrNAGS1* fruits was significantly elevated by 8.2-fold, resulting in an 89% increase in NAGS enzyme activity. Similarly, in OE-*RrADC1* fruits, the expression level of *RrADC1* was significantly enhanced by 3.5-fold, which was accompanied by a 70%

increase in ADC enzyme activity. Further analysis indicated that the levels of hydrolyzed arginine and free arginine in OE-*RrNAGS1* fruits rose by 15% and 100%, respectively. Conversely, in OE-*RrADC1* fruits, the contents of these two forms of arginine decreased by 17% and 34%, respectively (Fig. 3A-C).

Virus-induced gene silencing（VIGS）was used to study gene function. Compared to the empty vector control, the fruit treated with VIGS-*RrNAGS1* and VIGS-*RrADC1* showed a reduction of 50% and 60% in the gene expression levels of *RrNAGS1* and *RrADC1*, and a decrease in NAGS and ADC enzyme activities by 46% and 40% respectively. Furthermore, in fruit treated with VIGS-*RrNAGS1*, the levels of hydrolyzed arginine and free arginine decreased by 25% and 48%, respectively. Conversely, in fruit treated with VIGS-*RrADC1*, the levels of these two forms of arginine increased by 50% and 123%, respectively (Fig. 3D-F). These results confirm that *RrNAGS1* functions as a key gene in the arginine synthesis metabolism of *R. roxburghii* fruit, contributing to an increase in arginine content. In contrast, *RrADC1* serves as a critical gene in arginine catabolism, leading to a reduction in arginine content.

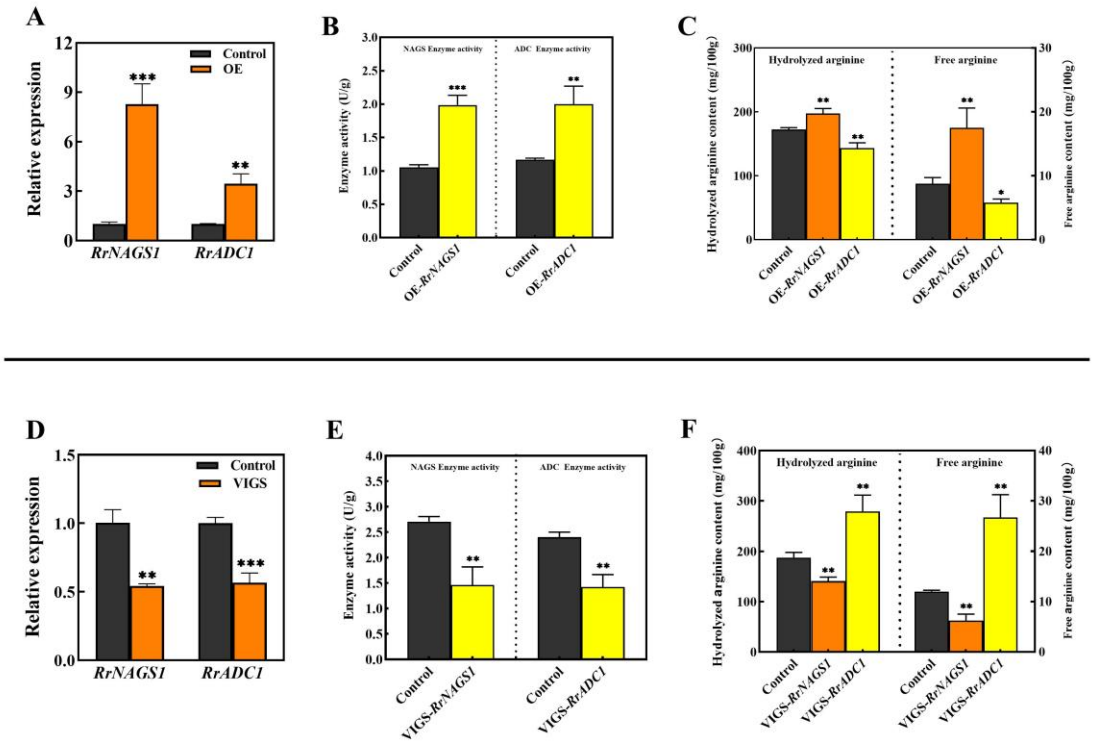

Fig.3. The transient overexpression and silencing of *RrNAGS1* and *RrADC1* correlate with the arginine content in *R. roxburghii* fruit.

(A) The expression of the *RrNAGS1* and *RrADC1* genes in *R. roxburghii* fruit was assessed by qRT-PCR. Control: pCAMBIA 1301; OE: 35S::*RrNAGS1*-Gus and 35S::*RrADC1*-Gus. (B) Enzyme activity in fruits transiently overexpressing *RrNAGS1* and *RrADC1*. (C) Hydrolyzed and free arginine contents in

fruits after transient overexpression of *RrNAGS1* and *RrADC1*. (D) qRT-PCR was used to analyze the transcription levels of *RrNAGS1* and *RrADC1* in the fruits after VIGS-induced gene silencing. Control: pTRV2; VIGS: VIGS-*RrNAGS1* and VIGS-*RrADC1*. (E) Impact of VIGS-mediated silencing of the *RrNAGS1* and *RrADC1* genes on enzyme activity in the fruits. (F) Impact of VIGS-mediated silencing of *RrNAGS1* and *RrADC1* genes on the contents of hydrolyzed and free arginine in the fruits. Data shown are mean ± SD of three independent biological replicates (n=3). The asterisk indicates statistical significance between treatments according to Tukey's test (*, $P < 0.05$; **, $P < 0.01$) (*, $P < 0.05$; **, $P < 0.01$).

3.4 Overexpression of *RrNAGS1* and *RrADC1* in strawberry fruits

Using the MEGA 7.0 bioinformatics software, we conducted a phylogenetic analysis of NAGS and ADC protein sequences from six species, including *R. roxburghii*, utilizing the Neighbor-Joining method. The results indicated that the *RrNAGS1* protein from *R. roxburghii* exhibits a high degree of homology with the *RcNAGS1* (XP 040370483.3) and *FvNAGS2* (XP 011466150.1) protein sequences (Fig. 4A). Similarly, the *RrADC1* protein also shows significant homology with the *RcADC* (XP 024167712.1) and *FvADC* (XP 004290299.1) protein sequences (Fig. 4B). Building upon these findings, we performed heterologous transient overexpression of *RrNAGS1* and *RrADC1* to investigate their functions in Strawberry fruit.

The results indicate that the overexpression of the *RrNAGS1* and *RrADC1* genes in strawberries, compared to the empty vector control group, significantly enhanced the expression levels of these two genes (Fig. 4C-D). This enhancement led to an 80% increase in NAGS enzyme activity and a 95% increase in ADC enzyme activity (Fig. 4E). Additionally, in fruits treated with OE-*RrNAGS1*, the content of hydrolyzed arginine and free arginine increased by 20 % and 48 % respectively. Whereas, fruits treated with OE-*RrADC1* exhibited a decrease in the content of these two forms of arginine by 5% and 27% respectively (Fig. 4F). These results suggest that the transient expression of the *RrNAGS1* gene in strawberry fruits significantly increases the content of hydrolyzed and free arginine, whereas the transient expression of the *RrADC1* gene results in a decrease in the content of hydrolyzed and free arginine.

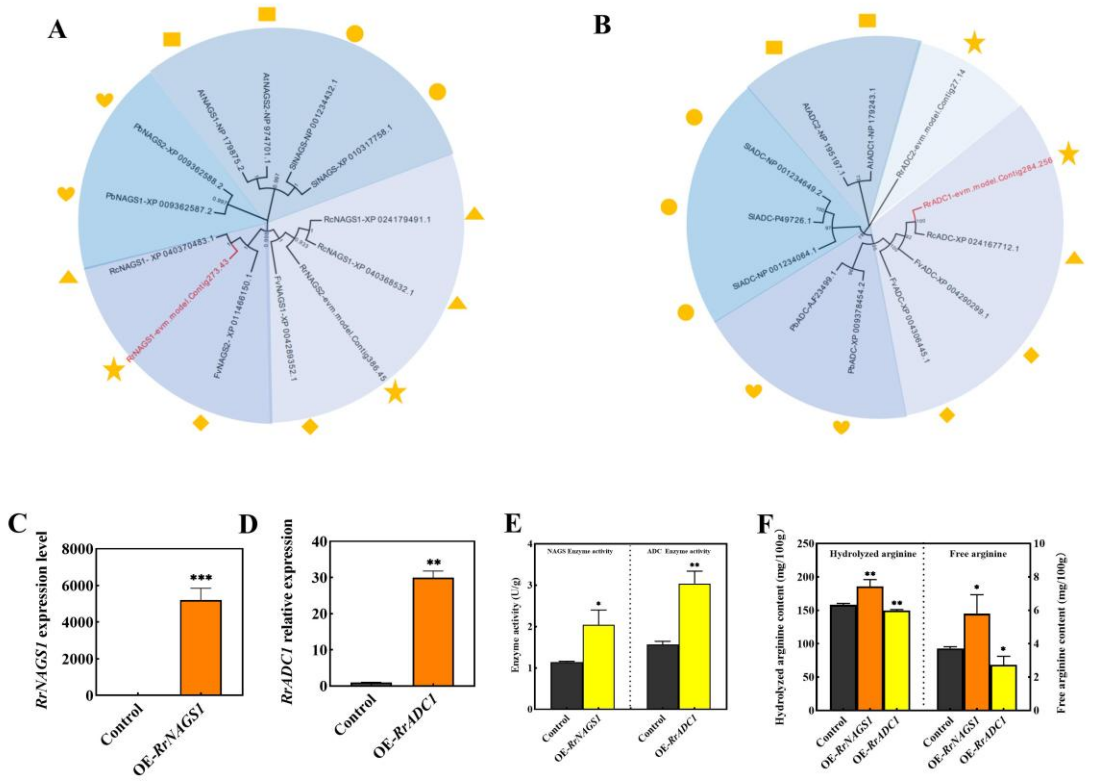

Fig.4. The heterologous transformation of *RrNAGS1* and *RrADC1*.

(A) Phylogenetic analysis of *RrNAGS1* proteins from other species. (B) Phylogenetic analysis of *RrADC1* proteins from other species. (C) The expression of *RrNAGS1* in strawberry was analyzed using qRT-PCR. Control represents the fruits containing an empty vector, while OE-*RrNAGS1* represents the fruits containing an overexpression vector. (D) The expression of the *RrADC1*gene in strawberry was analyzed using qRT-PCR. Control represents the fruits containing an empty vector, while OE-*RrADC1* represents the fruits containing an overexpression vector. (E) Enzyme activity of transient overexpression of *RrNAGS1* and *RrADC1*. (F) Arginine content of transient overexpression of *RrNAGS1* and *RrADC1*. Data shown are mean ± SD of three independent biological replicates (n=3). The asterisk indicates statistical significance between treatments according to Tukey's test. Rr: *R. roxburghii*, Rc: *Rosa chinensis*, Pb: *Pyrus x bretschneideri*, Fv: *Fragaria vesca* , Sl: *Solanum lycopersicum*, At: *Arabidopsis thaliana*.

3.5 RrLHY binds and activates the *RrNAGS1* promoter.

After confirming *RrNAGS1* and *RrADC1* as key genes involved in arginine metabolism, we analyzed their 2-kb upstream sequences and identified multiple binding sites for MYB transcription factors, indicating the significance of MYB in arginine accumulation (Fig. S2). Transcriptomic data were

336 employed to identify 13 RrMYBs associated with the expression of *RrNAGS1* and *RrADC1*. The analysis
337 revealed that evm.model.Contig191.1 (RrLHY, LATE ELONGATED HYPOCOTYL) exhibited a
338 significant positive correlation with *RrNAGS1* and an inverse correlation with *RrADC1* (Table S3). qRT-
339 PCR analysis revealed that the expression pattern of *RrLHY* across eight developmental stages of fruit
340 was consistent with that of *RrNAGS1* and arginine content (Fig. 5A). Consequently, *RrLHY* was
341 identified as a candidate gene for studying the regulation of arginine metabolism.

342 First, subcellular localization analysis suggested that RrLHY was a nucleus-localized protein
343 consistent with the proposed TF function (Fig. 5B). Furthermore, the yeast one-hybrid experiment
344 indicated that RrLHY binds to the *RrNAGS1* promoter (Fig.5C) but does not bind to the *RrADC1*
345 promoter (Fig. 5D). Additionally, luminescence intensity of the leaves are shown in Figure 5E. When
346 *35S::RrLHY*+pro*RrNAGS1*::LUC are co-expressed in the leaves, the luminescence intensity of D-
347 Luciferin is significantly higher than that of Empty vector+pro*RrNAGS1*::LUC. Moreover, the results of
348 a dual-luciferase assay in tobacco leaves (threshold set as 2) suggested that RrLHY activated the
349 *RrNAGS1* promoter, of approximately 2.2-fold (Fig. 5F). Next, *in vitro* experiments using electrophoretic
350 mobility shift assay (EMSA) revealed that RrLHY could directly recognize and bind to the AAATAT-
351 containing elements in the *RrNAGS1* promoter. When the specific AAATAT element was mutated by
352 CCCCCC sites, the putative RrLHY protein binding was eliminated. Meantime, the binding affinity of
353 the biotinylated probe was substantially reduced as the concentration of the competitor (cold probe)
354 increased (Fig. 5G). Collectively, these results revealed that RrLHY functions as a positive direct
355 regulator activating *RrNAGS*1 expression.

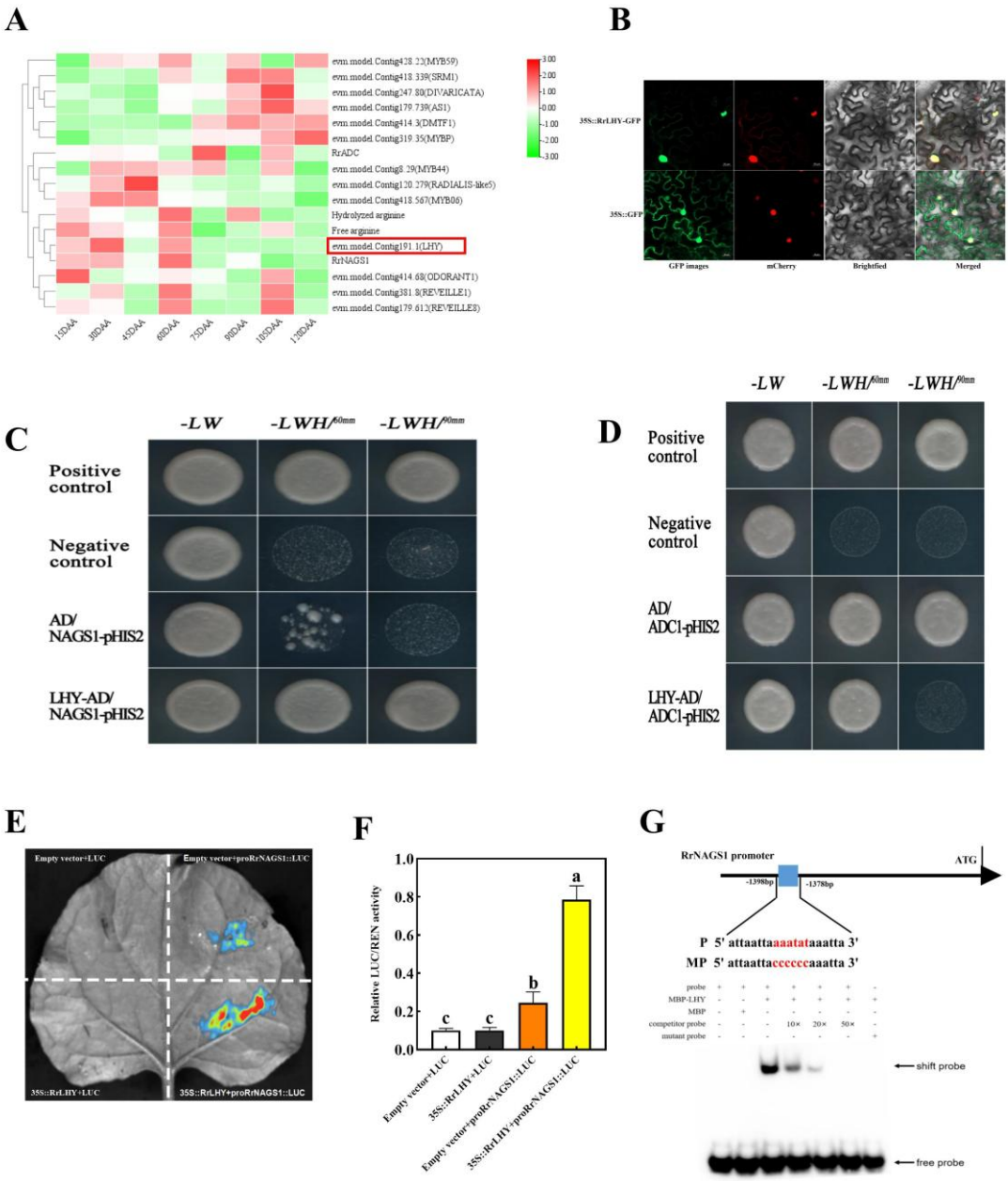

Fig.5. RrLHY Transcriptionally Activates *RrNAGS1*.

(A) Heatmap analysis of arginine content and the expression of 13 RrMYBs, *RrNAGS1*, and *RrADC1*. (B) Subcellular localization analysis of *RrLHY*. The fluorescent signals were detected in tobacco cells transfected with *RrLHY*-GFP and the nuclear RFP-NLS marker. Scale bar = 20 μm. (C) Yeast 1-hybrid analysis of RrLHY binding capacity to the *RrNAGS1* promoter, with the empty vector pGADT7 (AD) used as a negative control. (D) Yeast 1-hybrid analysis of RrLHY binding capacity to the *RrADC1* promoter, with the empty vector pGADT7 (AD) used as a negative control. (E) Transient transformation of tobacco leaves showing luminescence intensity. (F) The regulatory effect of RrLHY on the *RrNAGS1*

promoter, the LUC/REN value of the empty 35S vector on the *RrNAGS1* promoter was set to 1.0, and Se values were calculated using 3 biological replicates. Different letters indicate significant differences ($P < 0.05$) by Duncan's multiple range test. (G) *In vitro* binding ability of RrLHY to the *RrNAGS1* promoter performed by EMSA. The presence (+) or absence (−) of specific probes is marked. The black arrows become larger from left to right, indicating an increase in the concentration of competitive probes. MBP protein was used as a negative control.

3.6 Overexpression and silencing of *RrLHY* gene correlate with Arginine accumulation in *R. roxburghii*

To confirm the role of *RrLHY* in regulating arginine biosynthesis, we conducted experiments involving transient overexpression and virus-induced gene silencing (VIGS) in *R. roxburghii* fruits. The transient overexpression of *RrLHY* resulted in a significant increase in the expression of *RrNAGS1*, which in turn elevated both enzyme activity and arginine levels (Fig. 6A-D). In contrast, VIGS led to a decrease in *RrNAGS1* expression, enzyme activity, and arginine levels when *RrLHY* was silenced (Fig. 6E-H). These findings suggest that *RrLHY* plays a crucial role in modulating arginine biosynthesis by inducing the expression of *RrNAGS1*.

To validate our findings, we generated transgenic *R. roxburghii* callus that overexpresses *RrLHY*. The presence of the transgene in the OE-*RrLHY R. roxburghii* callus was confirmed via PCR (Fig. 7A). The OE-*RrLHY* transgenic lines demonstrated significantly elevated levels of *RrNAGS1*, enzyme activity, and arginine compared to the control (Fig. 7B-E). In conclusion, RrLHY exerts a specific regulatory effect on *RrNAGS1*, thereby promoting arginine accumulation.

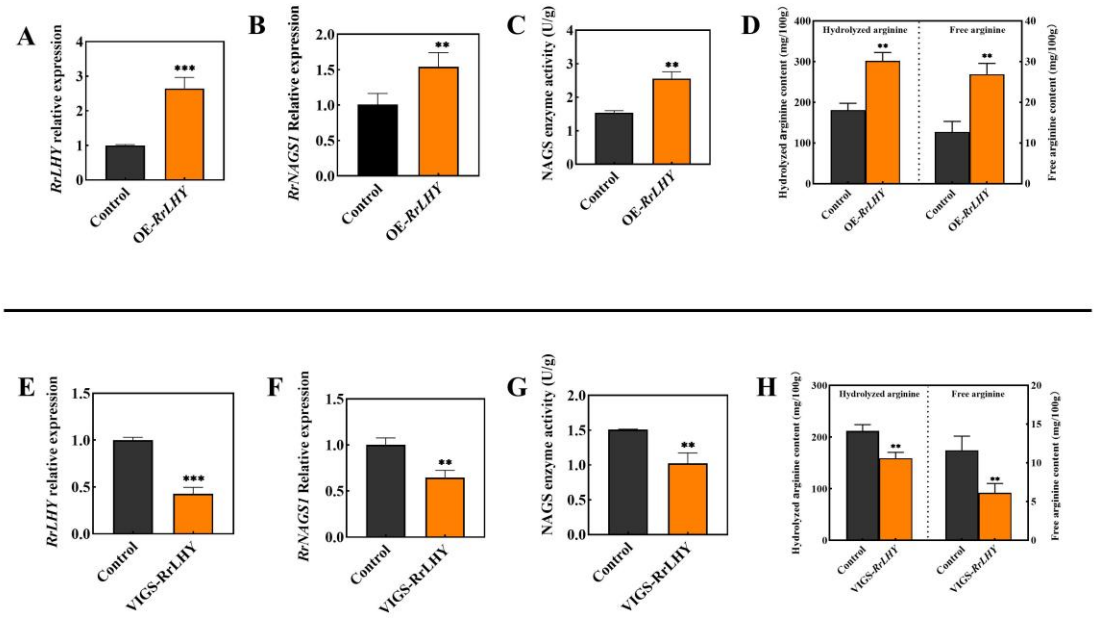

Fig.6. Effects of *RrLHY* overexpression and silencing on *RrNAGS1* Expression, NAGS Activity, and arginine content in *R. roxburghii* Fruits.

(A) The expression of the *RrLHY* gene in *R. roxburghii* fruit was analyzed using qRT-PCR. The control represents fruits containing an empty vector, while OE-*RrLHY* represents the fruits containing an overexpression vector. (B) Transcriptional level of *RrNAGS1* in fruits after transient overexpression of *RrLHY*. (C) NAGS enzyme activity in fruits after transient overexpression of *RrLHY*. (D) Effect of transient overexpression of *RrLHY* on the hydrolyzed and free arginine content in the fruits. (E) qRT-PCR was employed to analyze the transcription level of *RrLHY* in the fruits after VIGS-induced silencing of the gene. The fruits infected with an empty vector were referred to as Control, while the fruits infected with a silent vector were referred to as VIGS-*RrLHY*. (F) Transcriptional level of *RrNAGS1* in fruits after VIGS silences *RrLHY* gene. (G) Impact of VIGS-mediated silencing of the *RrLHY* gene on NAGS enzyme activity in the fruits. (H) Impact of VIGS-mediated silencing of the *RrLHY* gene on the contents of hydrolyzed and free arginine in the fruits. Data shown are mean ± SD of three independent biological replicates (n=3). Asterisks indicates statistical significance between treatments according to Tukey's test (*, $P < 0.05$; **, $P < 0.01$).

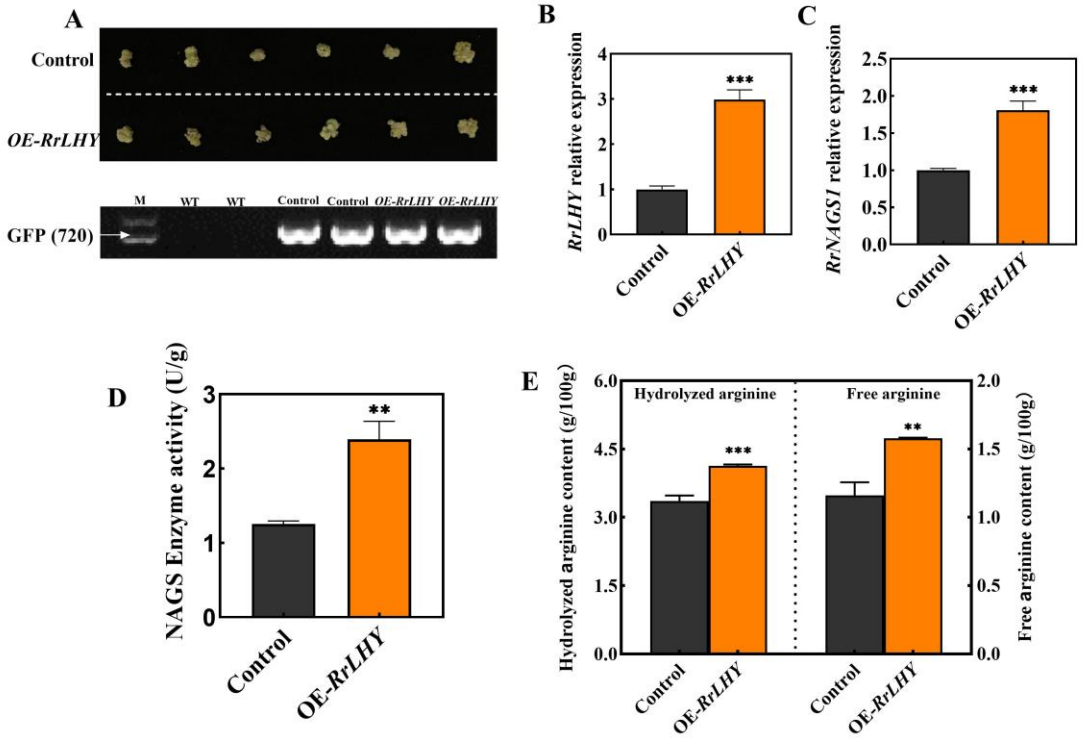

Figure.7. Stable overexpression of *RrLHY* increases arginine content in transgenic callus

(A) The phenotype of OE-*RrLHY* callus: M represents 2000 Marker; WT represents nontransgenic callus; Control represents the overexpression vector plasmid; and OE-*RrLHY* represents transgenic callus. (B) The expression of the *RrLHY* gene in *R. roxburghii* fruit was analyzed using qRT-PCR. Control represents the fruits containing an empty vector, while OE-*RrLHY* represents the fruits containing an overexpression vector. (C) Transcriptional level of *RrNAGS1* in fruits after transient overexpression of *RrLHY*. (D) NAGS enzyme activity in fruits after transient overexpression of *RrLHY*. (E) Effect of transient overexpression of *RrLHY* on the hydrolyzed and free arginine content in the fruits. Data showed are mean ± SD of three independent biological replicates (n=3). Asterisks indicates statistical significance between treatments according to Tukey's test (*, $P < 0.05$; **, $P < 0.01$).

4. Discussion

4.1 Changes in arginine content during the development of *R. roxburghii* fruits.

The content of metabolites in *R. roxburghii* Tratt fruits peak at different developmental stages. Specifically, the content of lignin, hemicellulose, cellulose, and pectin reach their maximum levels 30 DAA (Zhang et al., 2021), whereas organic acids, lipids, and ascorbic acid (ASA) peak at 90 DAA (Li et al., 2022; Lin et al., 2024). Notably, the concentrations of carotenoids, proanthocyanidins, phenolics, coumarins (Li et al., 2022), as well as arginine, total free glutamate, and total free amino acids, that are

the focus of this study, all reach their highest levels 60 DAA (Fig. 1C-1D). During this critical developmental period, the arginine content in fruit of *R. roxburghii* is significantly higher than that of mature fruits (120 DAA), indicating that this is the optimum stage for extracting these metabolites, to efficiently utilize these bioactive components and provide high-quality raw materials for the food and pharmaceutical industries.

Research on arginine accumulation during fruit development is relatively limited. Lv et al. (2020) found that free arginine decreases during the development of strawberry fruits. In this study, we investigated arginine in *R. roxburghii* fruits and discovered that the contents of free arginine and hydrolyzed arginine reached their peak at 60 DAA, followed by a downward, fluctuating trend that is consistent with the changes in glutamate and total amino acids. This is similar to the amino acid content changes observed during the fruit development of 'Yali' pears (Fan et al., 2020). Furthermore, environmental factors such as light, drought, and low temperature have been demonstrated to influence arginine levels in plants (Kc et al., 2021; Molesini et al., 2015; Mao et al., 2020). Consequently, we hypothesize that the accumulation of arginine in *R. roxburghii* fruits is not only associated with the developmental stage but may also be affected by external environmental factors.

4.2 *RrNAGS1 and RrADC1* are key genes in the arginine metabolic pathway during the development of *R. roxburghii* fruit.

The regulation of arginine levels is controlled by essential enzyme genes within this metabolic pathway (Slocum, 2005). Specifically, the *ASL* gene in rice, the *NAGK* gene in Arabidopsis, the *OTC* gene in watermelon, and the *ASS* gene in peanut are all critical to the regulation of arginine synthesis in their respective plant species (Xia et al., 2014a; Huang et al., 2017; Joshi et al., 2019; Li et al., 2022). In this study, we investigated the regulatory mechanisms underlying arginine synthesis in the fruit of *R. roxburghii.* We identified *RrNAGS1* as a crucial rate-limiting gene essential for this process within the fruit. By overexpressing *RrNAGS1* in both *R. roxburghii* and strawberry fruits, we observed a significant increase in arginine levels (Fig. 3C-4F). These findings are consistent with the research conducted by Kalamaki et al. (2009) and Mao et al. (2023), suggesting that the *NAGS1* gene likely performs similar functions across various plant species, including tomato fruits and rubber trees (*Hevea brasiliensis*). In addition, we examined the regulatory mechanisms underlying arginine catabolism. By overexpressing the key gene *RrADC1* in the fruits of *R. roxburghii* and strawberries, we observed a significant reduction in arginine content within the

fruits (Fig. 3F-4F). This finding is consistent with research conducted by Gao et al. (2021), which demonstrated that abscisic acid (ABA) can upregulate the *ADC* gene, leading to a reduction in arginine accumulation and promoting fruit ripening. Therefore, we can infer that *RrADC1* plays a crucial role in regulating arginine accumulation and facilitating the process of fruit ripening.

4.3 RrLHY increases arginine biosynthesis by controlling *RrNAGS1* transcription level

LHY is a MYB transcription factor that belongs to the *RVE* family, characterized by its SHAQKYF-type Myb DNA-binding domain (McClung et al., 2013). Recent studies have broadened the scope of *LHY* research beyond its established roles in regulating circadian rhythms (Wang et al., 2021), hormone signaling (Zhou et al., 2024), photoperiodic flowering (Fan et al., 2024), and stress responses (Lu et al., 2023), to include its influence on fruit quality. In spinach (*Spinacia oleracea*), SoLHY significantly influences the expression of the key ascorbic acid (ASA) synthesis gene *SoVTC2*, thus participating in the regulation of the ASA biosynthetic pathway (Thammawong et al., 2024). Under light-induced conditions, *LHY* contributes to the regulation of anthocyanin content in pepper (*Capsicum annuum*) and sweet cherry (*Prunus avium*), as well as affecting carotenoid metabolism in cucumber (*Cucumis sativus*) (Zhou et al., 2024; Zhang et al., 2023; Obel et al., 2022). In jasmine (*Jasminum sambac*), *JsLHY* regulates the transcription of genes involved in the aromatic biosynthetic pathway, thereby promoting the production of vinylphenol (VPB) and vinylphenolic acid (VT) (Zhou et al., 2024). However, the role of *LHY* in the arginine biosynthetic pathway has not yet been investigated. In this study, we used Yeast one-hybrid, dual-luciferase, and electrophoretic mobility shift assays (EMSA) to confirm that RrLHY activates the *RrNAGS1* promoter through binding to the AAATAT element (Fig. 5). This binding sequence aligns with those identified in Arabidopsis and soybean (Adams et al., 2018; Lu et al., 2020). Overexpression of *RrLHY* in fruit and callus tissues enhances *RrNAGS1* expression and promotes arginine accumulation (Figs. 6-7). In contrast, the correlation between *RrADC1* and *RrLHY* was found to be weak, with no interaction detected (Figs. 5A-D). Our findings indicate that RrLHY positively regulates the key enzyme gene *RrNAGS1* within the arginine biosynthetic pathway, thereby facilitating arginine synthesis.

During the analysis of transcriptomic data from *R. roxburghii* and qRT-PCR data across eight different fruit development stages (15-120 DAA), we found that the expression of the *RrLHY* gene peaked at the 30 DAA and 60 DAA stages. Concurrently, metabolites such as dietary fiber (including lignin, hemicellulose, cellulose, and pectin), proanthocyanidins, flavonoids, and total phenolics also

exhibited their highest content in the fruits at these specific stages (Zhang et al., 2021; Li et al., 2022). Additionally, according to the research report by Lu and Guo et al. (2020), specific steps in the ascorbic acid biosynthetic pathway exhibit rhythmic activity. Building on these findings, we hypothesize that the *RrLHY* gene may play a role in regulating the synthesis of these key metabolites in *R. roxburghii* fruits. Through the analysis of the cis-acting elements within the *RrLHY* promoter, we identified multiple elements that respond to light, hormones, and low-temperature stress. This finding suggests that *RrLHY* plays a significant regulatory role in the growth and development of *R. roxburghii*. Despite the significance of the LHY transcription factor, its regulatory functions in plant growth and development remain largely unexplored, especially concerning the formation of fruit quality. Further research is necessary to clarify the role of *LHY* in various biological processes in plants, thereby providing a theoretical foundation for the enhancement of fruit quality and nutritional value.

5. Conclusion

The quality of *R. roxburghii* fruit is closely linked to the accumulation of arginine, which is critically significant for the breeding of superior protein varieties. To investigate this mechanism in depth, this study successfully cloned two key structural genes that influence arginine accumulation in *R. roxburghii* fruit: *RrNAGS1* and *RrADC1*. Their functions were validated in both *R. roxburghii* and strawberry fruits, further confirming their roles. Additionally, we identified potential regulatory factors for *RrNAGS1*, revealing that RrLHY can directly activate the transcription of *RrNAGS1*. Through the overexpression of *RrLHY*, we observed a significant increase in the levels of free and hydrolyzed arginine in *R. roxburghii* fruit. Employing Y1H and EMSA analysis techniques, we confirmed that RrLHY can directly bind to the promoter of *RrNAGS1*, thereby regulating arginine synthesis in *R. roxburghii* fruit. These findings emphasize the immense potential of *R. roxburghii* fruit as a functional food and its application in food processing, providing a theoretical reference for cultivating *R. roxburghii* fruit varieties with improved quality and high arginine content.

CRediT authorship contribution statement

Xufeng Yang: Writing – original draft, Methodology, Investigation, Formal analysis, Data curation. **Nanyu Li:** Methodology, Data curation. **Richard Ludlow:** Methodology, Writing – review & editing . **Qianmin Hua:** Methodology, Data curation. **Zhaoxin Wu:** Investigation, Formal analysis. **Qinqian Yuan:** Investigation, Formal analysis. **Zhifa Li:** Investigation, Formal analysis. **Min Lu:** Writing – review & editing, Resources, Project administration, Methodology, Funding acquisition,

Conceptualization. **Huaming An:** Writing – review & editing, Resources, Project administration, Methodology, Funding acquisition, Conceptualization.

Declaration of Competing Interest

The authors declare that they have no known competing financial interests or personal relationships that could have appeared to influence the work reported in this paper.

Acknowledgments

This work was supported by the National Natural Science Foundation of China [Grant No 32060657].

Appendix A. Supplementary data

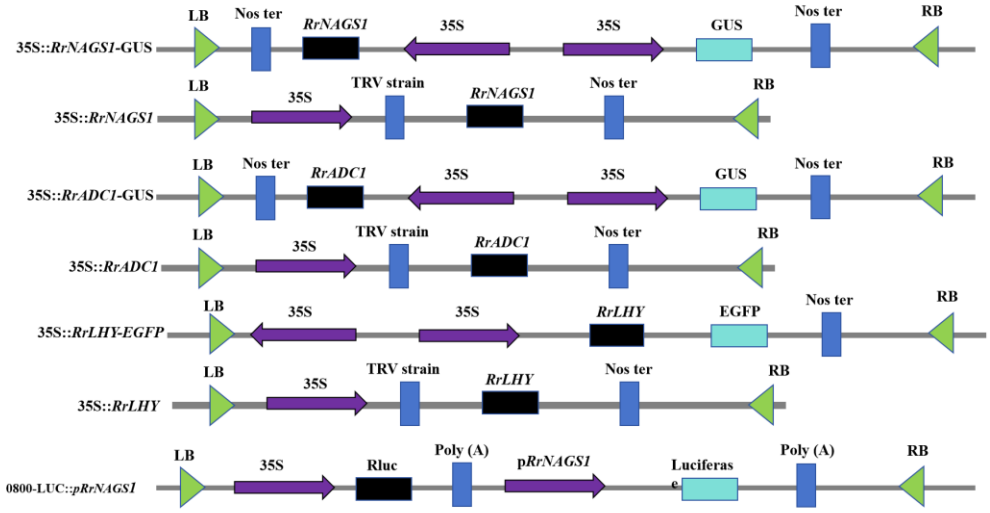

Supplemental Figure S1. Expression vectors for gene transformation.

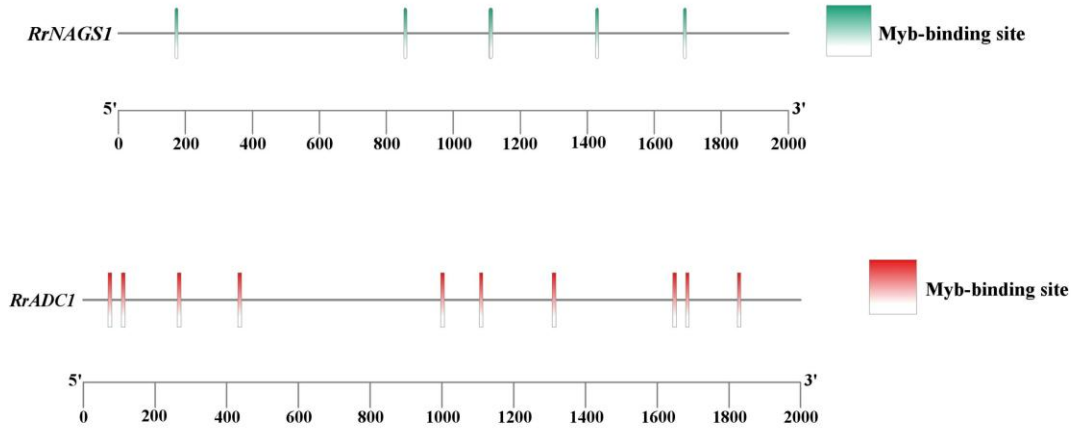

Supplemental Figure S2. Analysis of crisis-acting elements of *RrNAGS1* and *RrADC1* genes in *R.*

521 *roxburghii* .

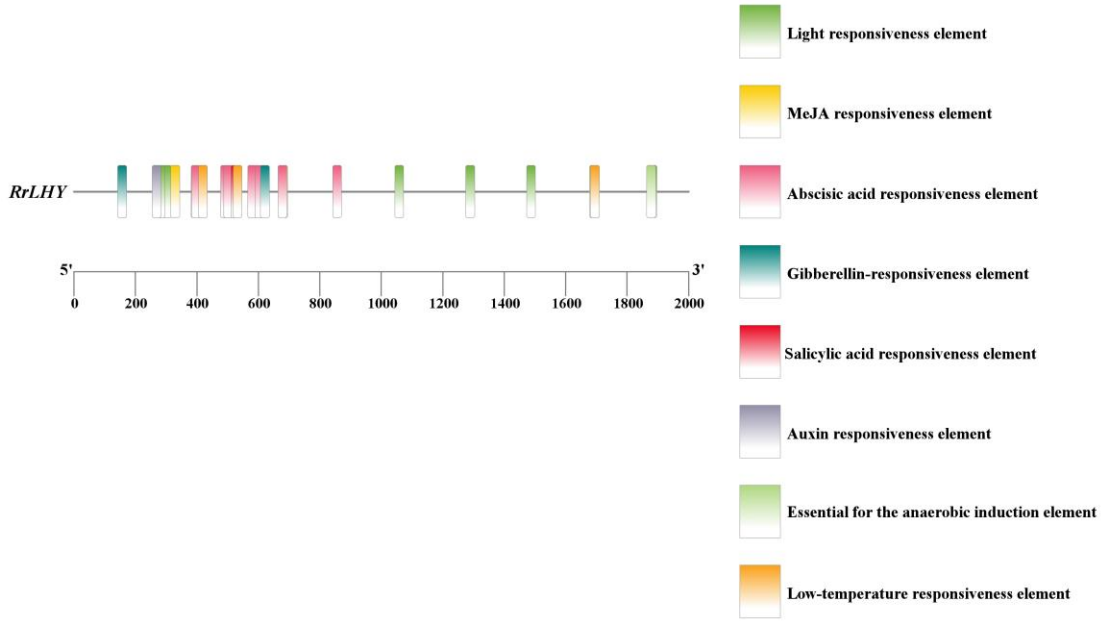

522

523 Supplemental Figure S2. Analysis of cis-acting elements of *RrLHY* genes in *R. roxburghii* .

524

525 Supplemental Table S1. Main Primers for experiments

Gene	Primer sequence (5'–3')	Usage
evm.model.Contig273.43	F: GAGTGATTACAACACAAGCCATGG R: CTTGAGCTACCGAGTACCTTTCTC	qRT-PCR
evm.model.Contig386.45	F: TGATGGATGACAGCGAGAGTGAC R: TCCAAGTGATGAGGGTCGTTCAC	qRT-PCR
evm.model.Contig144.322	F:GGAATTCTGGAGGATCGAGAGGATC R: TACTAGCAGTCCTCACTCCCTGAG	qRT-PCR
evm.model.Contig381.144	F: GACCAGGTTGAAGCAGTAGTTAGC R: AGCAGAGGTAGAGGATGTGTCAG	qRT-PCR
evm.model.Contig161.452	F: GTCAATTGCATCGGTGTTTCCTC R: GTAGACGGAAGTCAGCAGACAG	qRT-PCR
evm.model.Contig332.117	F: GGCAGGTCTGTATCTTTGCTGTG R: TGGAAGAACCGCTGAATTGTGG	qRT-PCR
evm.model.Contig257.173	F: CAGTCATTTCGATGAGCTGTGAC R: CCAGCAATTCGATCTCCATTCTC	qRT-PCR
evm.model.Contig80.183	F: TTCTGCGTACTGCTTGTGATGAG R: CAGCTAGTGGCTTAGCTAGTGTC	qRT-PCR
evm.model.Contig280.133	F: CGTCTCAGAGAAAGGTCAGTACTTC R: GAAGACCAGAATTCCTACAGGCATC	qRT-PCR
evm.model.Contig290.142	F: CTTCTGGGTTTAAGCCCACTCG R: CGAGAACAATCCCAACGTTCAAG	qRT-PCR
evm.model.Contig281.196	F: GGAGAATCTGATGAAGAGCGTTGAG R: GTTGCATGTTCATCGCATATCCATC	qRT-PCR
evm.model.Contig190.95	F: AATAGCATGGCCAGTAAAGCTCATG R: GAATCCTCCAAGTGAGGTGATGATC	qRT-PCR

evm.model.Contig209.216	F: CCATTGCAGGAGTTGGTGTG R: AAGCTTCCAAGGTATCGCTCC	qRT-PCR
evm.model.Contig120.291	F: TAGATAGAGCAGCGGAAGTGAAGG R: TGAAACACGAGTTCTCATGGATGG	qRT-PCR
evm.model.Contig21.5	F: CAGGCTGCGAAATTCTCACAG R: TCTCCATACCACGTGCAACTTC	qRT-PCR
evm.model.Contig284.27	F: TGAAGTTGCACGTGATATGGAGAAG R: GTTGTCAGAACTTCTCCACCTAACC	qRT-PCR
evm.model.Contig284.28	F: CTTGTTGGAGATCTTGCCAATGG R: GCACTTTCTTCCCACTCAACTTC	qRT-PCR
evm.model.Contig104.466	F: ATGCCTTGATGGAGTTGCATGTC R: CTTGGTTGCGAGCTCTAGTTACAC	qRT-PCR
evm.model.Contig104.465	F: ACTCTCCCTCAGACTCTTGAGTC R: AAGAAGCTTGGAGATTCTCTCGG	qRT-PCR
evm.model.Contig403.2	F: CGTCCTATTATTGCTAAGGCCATGG R: ATGTCAGCTCAAACCGAACCTGATC	qRT-PCR
evm.model.Contig238.10	F: GTTGAACAGCTTGAACGTGATGC R: CGATCGATTGGAAGTCCAGTGC	qRT-PCR
evm.model.Contig136.166	F: CGTGATGTTCTCAACATACTGCAC R: CATTGCAGTCATCCCATCAACAG	qRT-PCR
evm.model.Contig27.14	F: AGCTTGGCTTGTCTGGTTATGAAG R: TACAAGCTTCTGAACATGCTCTCTG	qRT-PCR
evm.model.Contig284.256	F: AGTACATCTCGCTGGCTCTGATG R: CAGAATGCTTGGTTCTGAGCTTCG	qRT-PCR
evm.model.Contig399.9	F: GTTCCAGGACATGCAGAAGGAG R: GTGCCTCGAATCGAACTCCTTC	qRT-PCR
evm.model.Contig191.1	F: GAACAAAGACTGCTGTGCAGATC R: ATGTTGGAGCAGCTTCACTAGAC	qRT-PCR
evm.model.Contig120.279	F: GGTGCAGGATCTCATGCATATAG R: AAGTAGAACTCGATACCTCTGTTC	qRT-PCR
evm.model.Contig428.22	F: CCTTGTGCTTGAGCTTCACTC R: CTTCTCTTGAGCCTTCTTCCTC	qRT-PCR
evm.model.Contig381.8	F: GATACAAGACCATGTTGGCAGC R: GTCAATGGGATCTGCAGAGCTTG	qRT-PCR
evm.model.Contig418.339	F: CATTCGCTTGAACTCGATGAATCG R: ATTGCTCTGTTGCCCTGTAATTGG	qRT-PCR
evm.model.Contig414.68	F: ATCAAGAGCAACAGCAACAAGAAG R: GAATCTCATGAGGCTCAATAAGTGG	qRT-PCR
evm.model.Contig8.29	F: GGAAGGAAATGGATCGGATCAAGG R: AGAGCTGGTTACACCATCTGAGAC	qRT-PCR
evm.model.Contig418.567	F: TCCTACCTTCCTCAGAGAACAGAC R: AATGTCTGTTTGGAGCCTTCTCTC	qRT-PCR
evm.model.Contig247.80	F: CTCAGTGATACCAGAACTCCATCTC R: ATGAACATGTTCCCATGAGCTTGAC	qRT-PCR
evm.model.Contig179.612	F: GTACATGCGATCCTAGTGGTATCG R: AGGAATACCATGGCTGACAGGAG	qRT-PCR
evm.model.Contig414.3	F: CGACATGGTACTCCATTGTAGATC R: CTTTCTCACCTCTTCGTACTCTTC	qRT-PCR
evm.model.Contig179.739	F: GGTAGAGTTGCAACTGGAATCG R: GCTTCGATCCTATCCAGAGCAG	qRT-PCR
evm.model.Contig319.35	F: CTGTCCACACTCTCAGTTCACAC R: CTTCAACACCTGGAGAGGAACTG	qRT-PCR

RrUBQ	F:ATGCAGATYTTTGTGAAGAC R: ACCACCACGRAGACGGAG	qRT-PCR
Action	*F: TGGGTTTGCTGGAGATGAT* *R: CAGTTAGGAGAACTGGGTGC*	qRT-PCR
RrEX84B	F:CTGTCATCTTGTGGCTTTCCGA R:TTGTAAGCCAAGAGGACCCAA	qRT-PCR

Gene	**Primer sequence (5'–3')**	**Usage**
RrNAGS1	F: ATGGCTACTCTAAGATCAAGGCTG R: GGAGACCACCACGACAAATGTC	Cloning
RrADC1	F: CAGACGTCCTCCGTGTGATG R: GCACGGCAATATGACCAGTC	Cloning
RrLHY	F: ATGGACAATTTCTCATCTGG R: GAATGTCAAGTTGAAGCCTCC	Cloning
OE-*RrNAGS1*	F: CGCGGTGGCGGCCGCTCTAGAGCAACAATGGCTACTCTAAGATC R: GATCTGCAGCCCGGGGGATCCAGGAAGATGGTGGATTGGGACTC	Gene Overexpression
OE-*RrADC1*	F: CGCGGTGGCGGCCGCTCTAGAATTAGATCGTCGCGGAAGAGATG R: GATCTGCAGCCCGGGGGATCCGCAGAACAAACCACCAACAACAG	Gene Overexpression
OE-*RrLHY*	F: ACGGGGGACGAGCTCGGTACCATGGACAATTTCTCATCTGGGG R: AACGATCCTGCAGCGACGCGTTCAAGTTGAAGCCTCCCCTTC	Gene Overexpression
VIGS-*RrNAGS1*	F: GTGAGTAAGGTTACCGAATTCATGGCTACTCTAAGATCAAGGCTG R: CGTGAGCTCGGTACCGGATCCGGAGACCACCACGACAAATGTC	Gene silencing
VIGS-*RrADC1*	F: GTGAGTAAGGTTACCGAATTCCAGACGTCCTCCGTGTGATG R: CGTGAGCTCGGTACCGGATCCGCACGGCAATATGACCAGTC	Gene silencing
VIGS-*RrLHY*	F: GTGAGTAAGGTTACCGAATTCACTAGCTTTAGCTGTCCTGTGCC R: CGTGAGCTCGGTACCGGATCCCAGTTGTTGCTAGGTCCTTCTCATT	Gene silencing
35S-*RrLHY*	F: ACGAACGATAGCCATGGTACCATGGACAATTTCTCATCTGGGG R: GCCTGCGGCCGCGCCGGATCCAGTTGAAGCCTCCCCTTCCA	Subcellular localization
p*RrLHY*	F: ACGGGGGACGAGCTCGGTACCATGGACAATTTCTCATCTGGGG R: AACGATCCTGCAGCGACGCGTTCAAGTTGAAGCCTCCCCTTC	Dual-luciferase
p*RrNAGS*	F: CTATAGGGCGAATTGGGTACCGAGTGAGAAGTAACATACAGGAGCATC R: GGGCTGCAGGAATTCGATATCATATAGCCTAGTAGCAGAAACGCG	Dual-luciferase
LHY-AD	F: TATGGCCATGGAGGCCAGTGAATTCATGGACAATTTCTCATCTG R: TCTGCAGCTCGAGCTCGATGGATCCTCAAGTTGAAGCCTCC	Y1H
NAGS1-phis2	F: ATACGACTCACTATAGGGCGAATTCGAGTGAGAAGTAACATAC R: ACCGCGGATCGATTCGCGAACGCGTATATAGCCTAGTAGCA	Y1H
ADC1-phis2	F: ATACGACTCACTATAGGGCGAATTCCCTCAAGACTTTCATGGACT R: ACCGCGGATCGATTCGCGAACGCGTCTCTTCCGCGACGATC	Y1H
MBP-LHY	F: GATCGGGCTCAGGGAGTGGTTCCGGCAGCGGCTCTGGATCGGCTGCCGCA GCAATTATGGACAATTTCTCATCTGGGGA R: ACTGCCGCCACTACCACCACCACTACCACCGCCTTTTTCAAACTGCGGAT GGCTCCAAGTTGAAGCCTCCCCTTCCAAG	EMSA
GFP	F: ATGGTGAGCAAGGGCGAGGA R: TTACTTGTACAGCTCGTCCA	transgenic testing

Supplemental Table S2. Structure genes of the regulated arginine accumulation

	correlation coefficient

gene ID	Annotation	metabolism	Free arginine	Hydrolyzed arginine	All arginine
evm.model.Contig273.43	*NAGS1*	anabolism	0.75*	0.815**	0.834**
evm.model.Contig386.45	*NAGS2*	anabolism	-0.576	-0.388	-0.414
evm.model.Contig144.322	*NAGK*	anabolism	-0.493	-0.604*	-0.614*
evm.model.Contig381.144	*NAGK*	anabolism	-0.633*	-0.217	-0.256
evm.model.Contig161.452	*ArgC*	anabolism	-0.586	-0.595	-0.612*
evm.model.Contig332.117	*ArgC*	anabolism	-0.536	-0.627*	-0.639*
evm.model.Contig257.173	*ArgD*	anabolism	-0.045	-0.274	-0.265
evm.model.Contig80.183	*ArgD*	anabolism	-0.454	-0.359	-0.377
evm.model.Contig280.133	*ArgD*	anabolism	-0.479	-0.185	-0.213
evm.model.Contig290.142	*ACY1*	anabolism	-0.116	-0.115	-0.118
evm.model.Contig281.196	*ACY1*	anabolism	-0.231	-0.254	-0.26
evm.model.Contig190.95	*ACY1*	anabolism	-0.056	-0.62	-0.595
evm.model.Contig209.216	*ArgE*	anabolism	-0.618*	-0.401	-0.429
evm.model.Contig120.291	*ArgF*	anabolism	0.17	0.314	0.313
evm.model.Contig21.5	*ArgF*	anabolism	-0.672*	-0.15	-0.194
evm.model.Contig284.27	*ArgF*	anabolism	-0.47	-0.534	-0.545
evm.model.Contig284.28	*ArgF*	anabolism	-0.523	-0.507	-0.523
evm.model.Contig104.466	*ArgG*	anabolism	-0.242	-0.583	-0.574
evm.model.Contig104.465	*ArgG*	anabolism	-0.372	-0.204	-0.223
evm.model.Contig403.2	*ArgG*	anabolism	-0.187	-0.28	-0.281
evm.model.Contig238.10	*ArgH*	anabolism	-0.308	0.006	-0.018
evm.model.Contig136.166	*Arg*	catabolism	-0.382	0.022	-0.008
evm.model.Contig284.256	*ADC1*	catabolism	-0.303	-0.653*	-0.646*
evm.model.Contig27.14	*ADC2*	catabolism	-0.697*	-0.559	-0.587
evm.model.Contig399.9	*NOS*	catabolism	-0.505	0.091	0.048

Note: * and ** represent significant difference at 0.05 and 0.01 levels, respectively.

Supplemental Table S3. Transcription factor of the regulated arginine accumulation

gene ID	Annotation	correlation coefficient	
		RrNAGS1	RrADC1
evm.model.Contig191.1	*RrLHY*	0.715	-0.905**
evm.model.Contig120.279	*RrRADIALIS-like 5*	0.761	-0.832*
evm.model.Contig428.22	*RrMYB59*	0.782	-0.825*
evm.model.Contig381.8	*RrREVEILLE 1*	0.831*	-0.803*
evm.model.Contig418.339	*RrSRM1*	0.820*	-0.797
evm.model.Contig414.68	*RrODORANT1*	0.856*	-0.77
evm.model.Contig8.29	*RrMYB44*	0.806*	-0.766
evm.model.Contig418.567	*RrMYB06*	0.857*	-0.756
evm.model.Contig247.80	*RrDIVARICATA*	0.84*	-0.752
evm.model.Contig179.612	*RrREVEILLE 8*	0.89*	-0.751
evm.model.Contig414.3	*RrDMTF1*	0.896*	-0.722
evm.model.Contig179.739	*RrAS1*	0.993**	-0.73
evm.model.Contig319.35	*RrMYBP*	-0.724	0.976**

Note: * and ** represent significant difference at 0.05 and 0.01 levels, respectively.

Data availability

Data will be made available on request.

Reference

Adams, S., Grundy, J., Veflingstad, S. R., Dyer, N. P., Hannah, M. A., Ott, S., & Carré, I. A. (2018). Circadian control of abscisic acid biosynthesis and signaling pathways revealed by genome-wide analysis of *LHY* binding targets. *The New phytologist*, *220*(3), 893–907. https://doi.org/10.1111/nph.15415.

Dai, H., Coleman, D. N., Lopes, M. G., Hu, L., Martinez-Cortés, I., Parys, C., Shen, X., & Loor, J. J. (2021). Alterations in immune and antioxidant gene networks by gamma-d-glutamyl-meso-diaminopimelic acid in bovine mammary epithelial cells are attenuated by in vitro supply of methionine and arginine. *Journal of dairy science*, 104(1), 776–785. https://doi.org/10.3168/jds.2020-19307.

Fan, J b., Zhang, S L., Ma, M., Liu, Z Q., Ren, Y Q., Wu, C Q., & Zhang, S L. (2020). Effects of bagging on the contents of free amino acids and hydrolyzed amino acids in 'Yali' pear fruit. *Acta Horticulturae Sinica* (02), 204-214. https://doi:10.13925/j.cnki.gsxb.20190256.

Fan, Y., Zhang, W., Zhang, J., Yang, T., Zhang, N., Liang, S., Dong, J., & Che, D. (2024). *RhLHY-RhTPPF-Tre6P* Inhibits Flowering in *Rosa hybrida* Under Insufficient Light by Regulating Sugar Distribution. *Plant, cell & environment*. Advance online publication. https://doi.org/10.1111/pce.15157.

Gambardella, J., Fiordelisi, A., Spigno, L., Boldrini, L., Lungonelli, G., Di Vaia, E., Santulli, G., Sorriento, D., Cerasuolo, F. A., Trimarco, V., & Iaccarino, G. (2021). Effects of Chronic Supplementation of L-Arginine on Physical Fitness in Water Polo Players. *Oxidative medicine and cellular longevity*, 2021, 6684568. https://doi.org/10.1155/2021/6684568.

Gao, F., Mei, X., Li, Y., Guo, J., & Shen, Y. (2021). Update on the Roles of Polyamines in Fleshy Fruit Ripening, Senescence, and Quality. *Frontiers in plant science*, *12*, 610313. https://doi.org/10.3389/fpls.2021.610313

Gao, W., Zhang, L., Wang, J., Liu, Z., Zhang, Y., Xue, C., Liu, M., & Zhao, J. (2021). *ZjSEP3* modulates flowering time by regulating the *LHY* promoter. *BMC plant biology*, *21*(1), 527. https://doi.org/10.1186/s12870-021-03305-x.

Gehrke, C.W., Wall Sr., L.L., Absheer, J.S., Kaiser, F.E., & Zumwalt, R.W., (1985). Sample preparation for chromatography of amino acids: Acid hydrolysis of proteins. *J Assoc Offical Anal Chem*, 68: 811– 821. https://doi.org/10.1093/jaoac/68.5.811.

He, J., Hou, T., Wang, Q., Wang, Q., Jiang, Y., Chen, L., Xu, J., Qi, Y., Jia, D., Gu, Y., Gao, L., Yu, Y., Wang, L., Kang, L., Si, J., Wang, L., & Chen, S. (2024). L-arginine metabolism ameliorates age-related cognitive impairment by Amuc_1100-mediated gut homeostasis maintaining. *Aging cell*, *23*(4), e14081. https://doi.org/10.1111/acel.14081.

Hiratsu, A., Tataka, Y., Namura, S., Nagayama, C., Hamada, Y., & Miyashita, M. (2022). The effects of acute and chronic oral l-arginine supplementation on exercise-induced ammonia accumulation and exercise performance in healthy young men: A randomised, double-blind, cross-over, placebo-controlled trial. *Journal of exercise science and fitness*, 20(2), 140–147. https://doi.org/10.1016/j.jesf.2022.02.003.

Hou, Z., Zhao, L., Wang, Y., & Liao, X. (2019). Effects of high pressure on activities and properties of superoxide dismutase from chestnut rose. *Food chemistry*, 294, 557–564. https://doi.org/10.1016/j.foodchem.2019.05.080.

Huang, J., Chen, D., Yan, H., Xie, F., Yu, Y., Zhang, L., Sun, M., & Peng, X. (2017). Acetylglutamate kinase is required for both gametophyte function and embryo development in Arabidopsis thaliana. *Journal of integrative plant biology*, *59*(9), 642–656. https://doi.org/10.1111/jipb.12536.

Jain, A., Sarsaiya, S., Gong, Q., Wu, Q., & Shi, J. (2024). Chemical diversity, traditional uses, and bioactivities of *Rosa roxburghii* Tratt: A comprehensive review. *Pharmacology & therapeutics*, 108657. https://doi.org/10.1016/j.pharmthera.2024.108657.

Joshi, V., Joshi, M., Silwal, D., Noonan, K., Rodriguez, S., & Penalosa, A. (2019). Systematized biosynthesis and catabolism regulate citrulline accumulation in watermelon. *Phytochemistry*, *162*, 129–140. https://doi.org/10.1016/j.phytochem.2019.03.003.

Kalamaki, M. S., Alexandrou, D., Lazari, D., Merkouropoulos, G., Fotopoulos, V., Pateraki, I., Aggelis, A., Carrillo-López, A., Rubio-Cabetas, M. J., & Kanellis, A. K. (2009). Over-expression of a tomato N-acetyl-L-glutamate synthase gene (*SlNAGS1*) in Arabidopsis thaliana results in high ornithine levels and increased tolerance in salt and drought stresses. *Journal of experimental botany*, *60*(6), 1859–1871. https://doi.org/10.1093/jxb/erp072.

Kc, S., Long, L., Liu, M., Zhang, Q., & Ruan, J. (2021). Light Intensity Modulates the Effect of Phosphate Limitation on Carbohydrates, Amino Acids, and Catechins in Tea Plants (*Camellia sinensis* L.). *Frontiers in plant science*, *12*, 743781. https://doi.org/10.3389/fpls.2021.743781

593 Kumar, S., Stecher, G., & Tamura, K. (2016). MEGA7: Molecular Evolutionary Genetics Analysis
594 Version 7.0 for Bigger Datasets. *Molecular biology and evolution*, 33(7), 1870–1874.
595 https://doi.org/10.1093/molbev/msw054.
596 Kyung, J., Jeon, M., Jeong, G., Shin, Y., Seo, E., Yu, J., Kim, H., Park, C. M., Hwang, D., & Lee, I.
597 (2022). The two clock proteins *CCA1* and *LHY* activate *VIN3* transcription during vernalization
598 through the vernalization-responsive cis-element. *The Plant cell*, *34*(3), 1020–1037.
599 https://doi.org/10.1093/plcell/koab304.
600 Lee, H. G., Won, J. H., Choi, Y. R., Lee, K., & Seo, P. J. (2020). Brassinosteroids Regulate Circadian
601 Oscillation via the *BES1/TPL-CCA1/LHY* Module in *Arabidopsisthaliana*. *iScience*, *23*(9), 101528.
602 https://doi.org/10.1016/j.isci.2020.101528.
603 Li, C., Lai, X., Luo, K., Zheng, Y., Liu, K., & Wan, X. (2022). Integrated metabolomic and transcriptomic
604 analyses of two peanut (*Arachis hypogaea* L.) cultivars differing in amino acid metabolism of
605 Li, H., Fang, W., Wang, Z., & Chen, Y. (2022). Physicochemical, biological properties, and flavour
606 profile of *Rosa roxburghii* Tratt, *Pyracantha fortuneana*, and *Rosa laevigata* Michx fruits: A
607 comprehensive review. *Food chemistry*, 366, 130509.
608 https://doi.org/10.1016/j.foodchem.2021.130509.
609 Li, N., Jiang, L., Liu, Y., Zou, S., Lu, M., & An, H. (2022). Metabolomics Combined with
610 Transcriptomics Analysis Revealed the Amino Acids, Phenolic Acids, and Flavonol Derivatives
611 Biosynthesis Network in Developing *Rosa roxburghii* Fruit. *Foods (Basel, Switzerland), 11*(11),
612 1639. https://doi.org/10.3390/foods11111639.
613 Lin, L., Zhang, S., Luo, L., Lu, M., & An, H. (2024). Structural feature of *RrGGP2* promoter and
614 functional analysis of *RrNAC56* regulating *RrGGP2* expression and ascorbate synthesis via stress-
615 inducible cis-elements in *Rosa roxburghii* Tratt. *International journal of biological macromolecules*,
616 *282*(Pt 1), 136584. Advance online publication. https://doi.org/10.1016/j.ijbiomac.2024.136584.
617 Liu, D. (2022). 1.17 Million Mu of *Rosa roxburghii* Tratt to Extend the Industrial Chain,
618 https://doi.org/10.28255/n.cnki.ngerb.2022.005506.
619 Lu, M., An, H., Wang, D. (2017). Characterization of Amino Acid Composition in Fruits of Three *Rosa*
620 *roxburghii* Genotypes. *Horticultural Plant Journal*, 3, 232-236.
621 https://doi.org/10.1016/j.hpj.2017.08.001.

622 Lu, M., Ma, W. T., Liu, Y. Q., An, H. M., & Ludlow, R. A. 2020. Transcriptome analysis reveals candidate
623 lignin-related genes and transcription factors in *Rosa roxburghii* during fruit ripening. *Plant*
624 *Molecular Biology Reporter*, 38, 331-342.https://doi.org/10.1007/s11105-020-01193-3.
625 Lu, S., Dong, L., Fang, C., Liu, S., Kong, L., Cheng, Q., Chen, L., Su, T., Nan, H., Zhang, D., Zhang, L.,
626 Wang, Z., Yang, Y., Yu, D., Liu, X., Yang, Q., Lin, X., Tang, Y., Zhao, X., Yang, X., … Kong, F.
627 (2020). Stepwise selection on homeologous *PRR* genes controlling flowering and maturity during
628 soybean domestication. *Nature genetics*, *52*(4), 428–436. https://doi.org/10.1038/s41588-020-0604-
629 7.
630 Lu, Y., & Guo, X. (2020). The Effect of Light in Vitamin C Metabolism Regulation and Accumulation
631 in Mung Bean (Vigna radiata) Germination. *Plant foods for human nutrition (Dordrecht,*
632 *Netherlands)*, 75(1), 24–29. https://doi.org/10.1007/s11130-019-00787-x.
633 Lu, Z., Liu, H., Kong, Y., Wen, L., Zhao, Y., Zhou, C., & Han, L. (2023). *Late Elongated Hypocotyl*
634 Positively Regulates Salt Stress Tolerance in *Medicago truncatula*. *International journal of*
635 *molecular sciences*, *24*(12), 9948. https://doi.org/10.3390/ijms24129948.
636 Lv, J., Pang, Q., Chen, X., Li, T., Fang, J., Lin, S., & Jia, H. (2020). Transcriptome analysis of strawberry
637 fruit in response to exogenous arginine. *Planta*, *252*(5), 82. https://doi.org/10.1007/s00425-020-
638 03489-w.
639 Mao, C., Li, L., Yang, T., Gui, M., Li, X., Zhang, F., Zhao, Q., & Wu, Y. (2023). Transcriptomics
640 integrated with widely targeted metabolomics reveals the cold resistance mechanism in *Hevea*
641 *brasiliensis*. *Frontiers in plant science*, *13*, 1092411. https://doi.org/10.3389/fpls.2022.1092411.
642 McClung C. R. (2013). Beyond Arabidopsis: the circadian clock in non-model plant species. *Seminars*
643 *in cell & developmental biology*, 24(5), 430–436. https://doi.org/10.1016/j.semcdb.2013.02.007.
644 McKay, T. B., Priyadarsini, S., Rowsey, T., & Karamichos, D. (2021). Arginine Supplementation
645 Promotes Extracellular Matrix and Metabolic Changes in Keratoconus. *Cells*, *10*(8), 2076.
646 https://doi.org/10.3390/cells10082076.
647 Min, D., Zhou, J., Li, J., Ai, W., Li, Z., Zhang, X., & Guo, Y. (2021). *SlMYC2* targeted regulation of
648 polyamines biosynthesis contributes to methyl jasmonate-induced chilling tolerance in tomato fruit.
649 *Postharvest Biology and Technology*, *174*, 111443.
650 https://doi.org/10.1016/j.postharvbio.2020.111443.

651 Molesini, B., Mennella, G., Martini, F., Francese, G., & Pandolfini, T. (2015). Involvement of the
652 Putative N-Acetylornithine Deacetylase from Arabidopsis thaliana in Flowering and Fruit
653 Development. *Plant & cell physiology*, *56*(6), 1084–1096. https://doi.org/10.1093/pcp/pcv030.
654 Obel, H. O., Cheng, C., Tian, Z., Njogu, M. K., Li, J., Du, S., Lou, Q., Zhou, J., Yu, X., Ogweno, J., &
655 Chen, J. (2022). Transcriptomic and Physiological Analyses Reveal Potential Genes Involved in
656 Photoperiod-Regulated β-Carotene Accumulation Mechanisms in the Endocarp of Cucumber
657 (*Cucumis sativus* L.) Fruit. *International journal of molecular sciences*, *23*(20), 12650.
658 https://doi.org/10.3390/ijms232012650.
659 Reis, M. E. M. D., Araújo, L. T. F., de Andrade, W. M. G., Resende, N. D. S., Lima, R. R. M., Nascimento,
660 E. S. D., Jr, Costa, M. S. M. O., & Cavalcante, J. C. (2018). Distribution of nitric oxide synthase in
661 the rock cavy (*Kerodon rupestris*) brain I: The diencephalon. *Brain research*, *1685*, 60–78.
662 https://doi.org/10.1016/j.brainres.2018.01.020.
663 Satriano J. (2004). Arginine pathways and the inflammatory response: interregulation of nitric oxide and
664 polyamines: review article. *Amino acids*, *26*(4), 321–329. https://doi.org/10.1007/s00726-004-
665 0078-4.
666 Shen, C., Wang, Y., Zhang, H., Li, W., Chen, W., Kuang, M., Song, Y., & Zhong, Z. (2023). Exploring
667 the active components and potential mechanisms of *Rosa roxburghii* Tratt in treating type 2 diabetes
668 mellitus based on UPLC-Q-exactive Orbitrap/MS and network pharmacology. *Chinese medicine*,
669 18(1), 12. https://doi.org/10.1186/s13020-023-00713-z
670 Shen, L., Wei, T., Zheng, L., Jiang, F., Ma, W., Lu, M., Wu, X., & An, H. (2023). Recent Advances on
671 Main Active Ingredients, Pharmacological Activities of *Rosa roxbughii* and Its Development and
672 Utilization. *Foods* (Basel, Switzerland), 12(5), 1051. https://doi.org/10.3390/foods12051051.
673 Slocum R. D. (2005). Genes, enzymes and regulation of arginine biosynthesis in plants. *Plant physiology*
674 *and biochemistry: PPB*, *43*(8), 729–745. https://doi.org/10.1016/j.plaphy.2005.06.007.
675 Song, J., Wu, H., He, F., Qu, J., Wang, Y., Li, C., & Liu, J. H. (2022). Citrus sinensis *CBF1* Functions in
676 Cold Tolerance by Modulating Putrescine Biosynthesis through Regulation of Arginine
677 Decarboxylase. *Plant & cell physiology*, *63*(1), 19–29. https://doi.org/10.1093/pcp/pcab135.
678 Thammawong, M. , Shomodder, A. , Kuroki, S. , Shiina, T. , Nagata, M. , & Nakano, K. . (2024). New
679 insights into the relationship between clock genes and ascorbic acid metabolism in spinach during

680 pre- and postharvest periods. *Postharvest Biology and Technology*, 216.
681 https://doi.org/10.1016/j.postharvbio.2024.113066.
682 the seeds. *Plant physiology and biochemistry*: *PPB*, 185, 132–143.
683 https://doi.org/10.1016/j.plaphy.2022.05.037.
684 Tran, P. V., Nguyen, L. T. N., Yang, H., Do, P. H., Torii, K., Putnam, G. L., Chowdhury, V. S., & Furuse,
685 M. (2020). Intracerebroventricular injection of L-arginine and D-arginine induces different effects
686 under an acute stressful condition. *Biochemical and biophysical research communications*, *533*(4),
687 965–970. https://doi.org/10.1016/j.bbrc.2020.09.111.
688 Wang, B., Liu, Y., Feng, L., Jiang, W. D., Kuang, S. Y., Jiang, J., Li, S. H., Tang, L., & Zhou, X. Q. (2015).
689 Effects of dietary arginine supplementation on growth performance, flesh quality, muscle
690 antioxidant capacity and antioxidant-related signalling molecule expression in young grass carp
691 (*Ctenopharyngodon idella*). *Food chemistry*, *167*, 91–99.
692 https://doi.org/10.1016/j.foodchem.2014.06.091.
693 Wang, K., Bu, T., Cheng, Q., Dong, L., Su, T., Chen, Z., Kong, F., Gong, Z., Liu, B., & Li, M. (2021).
694 Two homologous *LHY* pairs negatively control soybean drought tolerance by repressing the abscisic
695 acid responses. *The New phytologist*, *229*(5), 2660–2675. https://doi.org/10.1111/nph.17019.
696 Wang, L. T., Lv, M. J., An, J. Y., Fan, X. H., Dong, M. Z., Zhang, S. D., Wang, J. D., Wang, Y. Q., Cai,
697 Z. H., & Fu, Y. J. (2021). Botanical characteristics, phytochemistry and related biological activities
698 of *Rosa roxburghii* Tratt fruit, and its potential use in functional foods: a review. *Food & function*,
699 *12*(4), 1432–1451. https://doi.org/10.1039/d0fo02603d.
700 Wang, S., Sun, Q., Zhang, M., Yin, C., & Ni, M. (2021). *WRKY2* and *WRKY10* regulate the circadian
701 expression of *PIF4* during the day through interactions with *CCA1/LHY* and *phyB*. *Plant*
702 *communications, 3*(2), 100265. https://doi.org/10.1016/j.xplc.2021.100265.
703 Wang, Y., Xi, Z., Wang, X., Zhang, Y., Liu, Y., Yuan, S., Zhao, S., Sheng, J., & Meng, D. (2023).
704 Identification of *bHLH* family genes in Agaricus bisporus and transcriptional regulation of arginine
705 catabolism-related genes by *AbbHLH1* after harvest. *International journal of biological*
706 *macromolecules*, *226*, 496–509. https://doi.org/10.1016/j.ijbiomac.2022.12.059.
707 Winter, G., Todd, C. D., Trovato, M., Forlani, G., & Funck, D. (2015). Physiological implications of
708 arginine metabolism in plants. *Frontiers in plant science*, 6, 534.
709 https://doi.org/10.3389/fpls.2015.00534.

Wu, G., Meininger, C. J., McNeal, C. J., Bazer, F. W., & Rhoads, J. M. (2021). Role of L-Arginine in Nitric Oxide Synthesis and Health in Humans. *Advances in experimental medicine and biology*, 1332, 167–187. https://doi.org/10.1007/978-3-030-74180-8_10.

Wu, H., Li, M., Yang, X., Wei, Q., Sun, L., Zhao, J., & Shang, H. (2020). Extraction optimization, physicochemical properties and antioxidant and hypoglycemic activities of polysaccharides from roxburgh rose (*Rosa roxburghii Tratt*.) leaves. *International journal of biological macromolecules*, *165*(Pt A), 517–529. https://doi.org/10.1016/j.ijbiomac.2020.09.198.

Xia, J., Yamaji, N., & Ma, J. F. (2014). An appropriate concentration of arginine is required for normal root growth in rice. *Plant signaling & behavior*, *9*(4), e28717. https://doi.org/10.4161/psb.28717.

Yin, C., Zhang, Y., Zhang, L., Tian, Y., Zhong, X., Fang, X., ... & Tao, A. (2024). Exploring *Rosa roxburghii* Tratt polysaccharides: From extraction to application potential in functional products-An in-depth review. *International Journal of Biological Macromolecules*, 135543. https://doi.org/10.1016/j.ijbiomac.2024.135543.

Yin, C., Zhang, Y., Zhang, L., Tian, Y., Zhong, X., Fang, X., Yang, Y., & Tao, A. (2024). Exploring Rosa roxburghii Tratt polysaccharides: From extraction to application potential in functional products - An in-depth review. *International journal of biological macromolecules*, 280(Pt 1), 135543. Advance online publication. https://doi.org/10.1016/j.ijbiomac.2024.135543.

Yu, L., Zhao, Z., Zhang, W., Ren, T. (2021). Comparative comprehensive quality analysis of rosa roxburghii fruit from different regions in Guizhou province, *Mod. Food Sci. Technol*, 37 (09) 169–178, https://doi.org/10.13982/j. mfst.1673-9078.2021.7.0041.

Zhang, P., & Hu, X. (2018). Metabolic engineering of arginine permeases to reduce the formation of urea in Saccharomyces cerevisiae. *World journal of microbiology & biotechnology*, *34*(3), 47. https://doi.org/10.1007/s11274-018-2430-y.

Zhang, X., Lu, M., Ludlow, R. A., Ma, W., & An, H. (2021). Transcriptome analysis reveals candidate genes for dietary fiber metabolism in *Rosa roxburghii* fruit grown under different light intensities. *Horticulture, Environment, and Biotechnology*, 62(5), 751-764. http://doi.org/10.1007/s13580-021-00359-6.

Zhang, Y., Chen, C., Cui, Y., Du, Q., Tang, W., Yang, W., Kou, G., Tang, W., Chen, H., & Gong, R. (2023). Potential regulatory genes of light induced anthocyanin accumulation in sweet cherry identified by

739 combining transcriptome and metabolome analysis. *Frontiers in plant science*, *14*, 1238624.
740 https://doi.org/10.3389/fpls.2023.1238624.
741 Zhou, C., Tian, C., Wen, S., Yang, N., Zhang, C., Zheng, A., Tan, J., Jiang, L., Zhu, C., Lai, Z., Lin, Y.,
742 & Guo, Y. (2023). Multiomics Analysis Reveals the Involvement of *JsLHY* in Controlling Aroma
743 Production in Jasmine Flowers. Journal of agricultural and food chemistry,
744 10.1021/acs.jafc.3c05768. *Advance online publication*. https://doi.org/10.1021/acs.jafc.3c05768.
745 Zhou, W., Xiao, R. Y., Yang, Y. X., Wang, X., Wang, D. H., & Wang, Z. Z. (2024). Clock protein *LHY*
746 targets *SNAT1* and negatively regulates the biosynthesis of melatonin in Hypericum perforatum.
747 *Science advances*, 10(38), eadq6505. https://doi.org/10.1126/sciadv.adq6505.
748 Zhou, Y., Wu, W., Sun, Y., Shen, Y., Mao, L., Dai, Y., Yang, B., & Liu, Z. (2024). Integrated transcriptome
749 and metabolome analysis reveals anthocyanin biosynthesis mechanisms in pepper (*Capsicum*
750 *annuum* L.) leaves under continuous blue light irradiation. *BMC plant biology*, 24(1), 210.
751 https://doi.org/10.1186/s12870-024-04888-x.